



# Testing the influence of light on nitrite cycling in the eastern tropical North Pacific

Nicole M. Travis<sup>1</sup>, Colette L. Kelly<sup>1</sup>, Karen L. Casciotti<sup>1,2</sup>

5 <sup>1</sup>Earth System Science, Stanford University, Stanford CA 94305 USA

<sup>2</sup>Oceans Department, Stanford University, Stanford CA 94305 USA

*Correspondence to: Nicole M. Travis (ntravis@stanford.edu)*

10 **Abstract.** Light is considered a strong controlling factor on nitrification rates in the surface ocean. Previous work has shown that ammonia oxidation and nitrite oxidation may be inhibited by high light levels, yet active nitrification has been measured in the sunlit surface ocean. While it is known that photosynthetically active radiation (PAR) influences microbial nitrite production and consumption, the level of inhibition of nitrification is variable across datasets. Additionally, phytoplankton have light-dependent mechanisms for nitrite production and consumption that co-occur with nitrification around the depths of the primary nitrite maximum (PNM). In this work, we experimentally determined the direct influence of light level on net nitrite production, including  
15 all major nitrite cycling processes (ammonia oxidation, nitrite oxidation, nitrate reduction, nitrite uptake) in microbial communities collected from the base of the euphotic zone. We found that although ammonia oxidation was inhibited at the depth of the PNM and was further inhibited by increasing light at all stations, it remained the dominant nitrite production process at most stations and treatments, even up to 25% surface PAR. Nitrate addition did not enhance ammonia oxidation in our experiments, but may have increased nitrate and nitrite uptake at a coastal station. In contrast to ammonia oxidation, nitrite oxidation was not clearly inhibited  
20 by light, and sometimes even increased at higher light levels. Thus, accumulation of nitrite at the PNM may be modulated by changes in light, but light perturbations did not exclude nitrification from the surface ocean. Nitrite uptake and nitrate reduction were both enhanced in high light treatments relative to low light, and in some cases showed high rates in the dark. Overall, net nitrite production rates of PNM communities were highest in the dark treatments.

## 1 Introduction

25 Accumulation of nitrite in the surface ocean in the primary nitrite maximum (PNM) is controlled by four dominant microbial processes, including ammonia oxidation, nitrite oxidation, nitrate reduction and nitrite uptake. The nitrification processes (ammonia oxidation and nitrite oxidation) are performed by specialized archaeal and bacterial cells, while nitrate reduction and nitrite uptake are largely light-dependent phytoplankton processes. Activity from these microbial groups has been measured near the PNM feature, but it is unclear what environmental conditions control the relative rates of these four microbial processes and  
30 the resulting concentrations of nitrite.

Light is an environmental parameter often suggested to control nitrification rates. Observed nitrification rates in ocean profiles are typically low in surface waters and increase to maximum rates at the base of the euphotic zone (Ward, 1985). These correlative



35 patterns across depth suggest that nitrification is inhibited by light. In the eastern tropical North Pacific ocean (ETNP), paired  
nitrification measurements (ammonia oxidation and nitrite oxidation) showed patterns where low light levels (<5% surface PAR)  
corresponded to the majority of high nitrification rates (>10 nM d<sup>-1</sup>) in the ETNP, although active nitrification was still occasionally  
measured in samples with light levels >10% surface PAR (Travis et al., 2023). 06/04/2023 07:37:00 Other work in the ETNP has  
shown ammonia oxidation rates are excluded from light levels above ~1-5% of surface PAR (Beman et al., 2012), while data from  
Monterey Bay, CA showed rates up to 35 nM d<sup>-1</sup> even at >90% surface PAR (Ward, 2005). Direct light inhibition has also been  
40 confirmed in cultured marine ammonia-oxidizing archaea (Merbt et al., 2012) and the marine nitrite-oxidizing bacteria *Nitrococcus*  
*mobilis* and *Nitrobacter sp.* (Guerrero and Jones, 1996a, b).

Differential light inhibition is a common theory posited to cause imbalance in the two steps of nitrification resulting in accumulation  
of nitrite (Brandhorst, 1958; Francis et al., 2005; Guerrero and Jones, 1996a, b; Hooper and Terry, 1974; Lomas and Lipschultz,  
45 2006; Mackey et al., 2011; Meeder et al., 2012; Merbt et al., 2012; Olson, 1981a). In order for differential light inhibition of  
nitrifiers to cause an imbalance leading to nitrite accumulation, nitrite-oxidizing bacteria would have to be more light-sensitive  
than ammonia oxidizers. Prior studies have shown that nitrifiers are light sensitive, but there is a lack of consensus on whether  
nitrite oxidizers (Olson, 1981a) or ammonia oxidizers are more photosensitive (Guerrero and Jones, 1996a; Hooper and Terry,  
1974; Horrigan and Springer, 1990). At the same time, measurements of ammonia oxidation and nitrite oxidation in the field are  
50 rarely in balance. It is also likely that light sensitivities are modulated by other environmental conditions; for example, substrate  
replete conditions and optimal temperatures are known to mitigate light sensitivity in some microbes. Recent work has suggested  
that instead of direct light inhibition, observed decreases in ammonia oxidation rate in near-surface waters could be attributable to  
increased competition with phytoplankton for substrates (Smith et al., 2014; Wan et al., 2018). This competition for ammonium  
has been postulated to be modulated by nitrate availability and light, where increased light causes increased ammonium affinity in  
55 phytoplankton and simultaneous declines in ammonium affinity for ammonia oxidation, giving phytoplankton a distinct advantage,  
especially in low-nutrient environments (Xu et al., 2019).

Phytoplankton are also influenced by light, with enhanced growth and N uptake at higher light levels. They have been observed to  
release nitrite under variable light and nutrient conditions (Collos, 1998; Kiefer et al., 1976; Lomas and Glibert, 2000; Lomas et  
60 al., 1999; Sciandra and Amara, 1994; Vaccaro and Ryther, 1960; Wada and Hattori, 1971). The physiological cause of nitrite  
release from phytoplankton is unclear, but it has been linked to nitrate uptake activity in dark and low light conditions and was  
attributed to incomplete nitrate assimilation (Vaccaro and Ryther, 1960; Kiefer et al., 1976). Other studies suggest that sporadic  
high light events stimulate excess nitrate reduction as a photosynthetic energy dissipation pathway (Lomas and Glibert, 1999;  
Lomas et al., 1999).

65 Many phytoplankton are also capable of nitrite uptake, although low availability of nitrite in the field can make using nitrite less  
favorable than using nitrate. Nitrate uptake rates are generally higher than those of nitrite uptake for many phytoplankton when  
both substrates are available (Collos, 1998). Nitrite reduction is an energy intensive process, and adequate light availability  
typically controls nitrite uptake (Collos and Berges, 2003; Berges, 1997; Berges and Harrison, 1995; Berges et al., 1995; Hattori  
70 and Wada, 1971; Lomas and Glibert, 2000). Wada and Hattori (1971) measured nitrite uptake in dark and light bottles in the ETNP,  
and confirmed that field assemblages take up more nitrite under higher light conditions. Thus, photosynthetic microbes are a  
relatively cryptic source of nitrite to the PNM because they are capable of both nitrite production and consumption. This dual



75 function as a source and sink term for nitrite allows phytoplankton to control nitrite accumulation on their own, or to become a competitor for the substrates required in nitrification (Smith et al., 2014; Wan et al., 2018). It can be difficult to discern what controls whether phytoplankton communities act as a net source or sink of nitrite in the field.

80 Both the uncoupling of the two steps of nitrification and nitrite release by phytoplankton (via nitrate reduction) have been used independently to explain PNM formation. However, it is likely that these processes co-occur (Wan et al., 2021). The relative rates of each process are controlled by the ecophysiological response of each microbial group to environmental conditions, leading to dynamic changes in net accumulation of nitrite (Carlucci et al., 1970). Few direct measurements attempt to separate all of the relevant, overlapping nitrite consumption and production rates in the field (Kiefer et al., 1976; Olson, 1981b; Travis et al., 2023). Experimental manipulations of light and nitrate availability are needed to understand the controls that regulate the balances between source and sink processes and between phytoplankton and nitrifier processes, and to separate the effects of microbial community composition from direct impacts of light and nutrients on the measured rates of these essential reactions.

85 In this study, we used natural microbial populations collected from PNM depths to experimentally determine the influence of light level and nitrate concentration on the relative rates of the four dominant microbial processes influencing nitrite accumulation. Our experimental manipulations provided insight into the physiological responses of the community that are distinct from conclusions obtained from the natural distributions of instantaneous rates across environmental gradients. Instantaneous rate distributions are reflections of the ambient environmental conditions (including light level), in addition to the natural community composition, whereas experimental manipulations illustrate responses of a specific community to environmental perturbations. We hypothesized that increased light intensity would lead to a shift towards higher phytoplankton activity and lower nitrification rates. We expected net nitrite production to decline at higher light levels, with nitrate reduction becoming a larger proportion of net production as ammonia oxidation rates declined. We also expected nitrate addition to cause an increase in phytoplankton nitrate uptake and a corresponding increase in ammonia oxidation rates through alleviation of substrate competition (Wan et al., 2021).

## 2 Methods

### 2.1 Site description and experimental design

100 Data were collected aboard the *R/V Sally Ride* (SR1805) from March to April 2018 and aboard the *R/V Falkor* (FK180624) from June to July 2018 in the Eastern Tropical North Pacific (ETNP). The SR1805 cruise transect spanned a straight path from near the western edge of the ETNP oxygen deficient zone (ODZ) at an offshore process station (PS1, 10°N, 113°W) towards a coastal process station (PS3, 17.7°N, 102.4°W) where experimental rates measurements were conducted. An additional process station was occupied near the geographic center of the oxygen deficient zone (PS2, 15.8°N, 105°W) (Fig. 1). While this study focused on euphotic zone processes, the region is underlain by a functionally anoxic zone, which was the focus of related studies (eg. Kelly et al., 2021; Sun et al., 2021; Frey et al., 2023). Hydrographic data were collected at each station using a Seabird SBE 911+ CTD package mounted either on a 12 or 24 Niskin bottle rosette (Temperature, Salinity, Pressure). Fluorescence data and photosynthetically active radiation (PAR) were collected using sensors on the 12-bottle rosette at each of the stations (PS1, PS2 and PS3). The FK180624 cruise transect occupied stations along 14°N latitude from ~102°W to ~116°W (Fig. 1). Experimental rate measurements were made at Station 2 (14°N, 103°W) and Station 9 (14°N, 110°W). Hydrographic data were collected at each



110 station using Seabird SBE 911+ CTD package mounted on a 12 Niskin bottle rosette. A 150-mL polycarbonate (PC) bottle was triple-rinsed and used to collect discrete samples for ambient source water dissolved inorganic nitrogen (DIN, including  $\text{NO}_3^-$ ,  $\text{NO}_2^-$ , and  $\text{NH}_4^+$ ) concentration measurements at each station and depth.

To determine the influence of light and nitrate concentration on microbial nitrite cycling, source water was collected from the lower slope of the PNM at experimental stations during a pre-dawn cast. Where available, nitrite concentration data from a previous cast were used to target the depth of the PNM at a given station; otherwise, the depth of the lower slope of the chlorophyll maximum guided water collection depths. Each source water community was incubated at four light levels, with and without an additional 20  $\mu\text{M}$  nitrate ( $\text{KNO}_3$ ). Low-light (LL), medium-light (ML) and high-light (HL) treatments (approximately 1%, 4% and 20% surface irradiance, sPAR) were achieved in flow-through seawater incubators with layered window-screening designed to maintain irradiance at the desired levels. A dark (DK) treatment was achieved using brown HDPE bottles and incubating in the 1% sPAR tank. Light levels in each incubator were directly measured during the cruise using a LicoR submersible PAR meter or a submerged HOBO LUX data logger. The deck-board incubation tank was continuously fed with surface seawater to maintain consistent temperature.

## 125 2.2 Rate measurements

Samples for rate measurements were collected directly from the Niskin bottles by triple rinsing and filling replicate experimental containers. Experimental bottles included 500-mL high-density brown polyethylene (HDPE) bottles for dark-incubated treatments, and corresponding 500-mL clear polycarbonate (PC) bottles for light-incubated experiments.  $^{15}\text{N}$  tracer appropriate for each process was then added to replicate incubation bottles: ammonia oxidation (98.8 *atm%*  $^{15}\text{N}$ - $\text{NH}_4\text{Cl}$ ), nitrate reduction (98.8 *atm%*  $^{15}\text{N}$ - $\text{KNO}_3$ ), and nitrite oxidation/uptake (98.8 *atm%*  $^{15}\text{N}$ - $\text{NaNO}_2$ ) (Sigma-Aldrich). At the coastal station PS3, uptake of ammonium and nitrate were also measured using  $^{15}\text{N}$ - $\text{NH}_4\text{Cl}$  and  $^{15}\text{N}$ - $\text{KNO}_3$  tracers, respectively. The appropriate  $^{15}\text{N}$  tracer solution was added at the start of each incubation to reach 200 nM  $^{15}\text{N}$  for all experiments and gently mixed. For experimental treatments with added nitrate, 20  $\mu\text{M}$  of unlabeled  $\text{KNO}_3$  solution was added to the incubation bottle.

135 Rate estimates are susceptible to stimulation from the  $^{15}\text{N}$  additions used to track transformation of substrate into the product pools. Tracer experiments often aim for 10%  $^{15}\text{N}$  addition to minimize rate stimulation from the added nitrogen, but this method relies on the substrate pool being large enough to consistently add  $^{15}\text{N}$  at  $\sim 10\%$  levels, which is impractical in regions where nitrogen concentrations are highly variable or very low. The determination of rates also depends on the assumptions that the labeled fraction of source DIN remains constant, and only a small percentage of the  $^{15}\text{N}$ -labeled source pool ends up in the product. If consumption of the source DIN is complete (i.e., 100% of  $^{15}\text{N}$  spike ends in the product), this can lead to an underestimate of the rate. Dilution of the source DIN pool during the course of the experiment (e.g., regeneration of ammonium from grazers) will also lead to underestimation of rates, especially over the course of longer incubation times. In this study, the addition of  $^{15}\text{N}$  at a uniform level of 200 nM across all experiments was the most feasible design for implementation across multiple cruises, stations, depths, and  
140  
145 DIN sources where nitrogen concentrations were variable. Given this, our  $^{15}\text{N}$  spikes ranged from  $<1\%$  to  $>90\%$  of the source nitrogen pool, and have the potential of stimulating the measured rates, especially in the higher % enrichment experiments. The potential enhancement of rates does not preclude comparison of light treatment effects.



150 After the  $^{15}\text{N}$  spike was added, a subsample was immediately filtered (Sterivex, 0.22  $\mu\text{m}$  pore size syringe filter) into a 60-mL HDPE bottle and frozen at  $-20^\circ\text{C}$  to represent initial conditions for later isotope analysis and nitrate concentration measurements upon return to Stanford University. An aliquot of each initial sample was also analyzed shipboard for ammonium and nitrite concentrations to confirm 200 nM  $^{15}\text{N}$  additions. At timepoints approximately 8-hours, 16-hours and 24-hours from initial spike time, a subsample was Sterivex-filtered (0.22  $\mu\text{m}$  pore size) into a 60-mL HDPE bottle and frozen for later isotope analyses and rate calculations. At the 24-hour time point, the remaining incubation water was combined from experimental replicates (to maximize particulate nitrogen content) and vacuum-filtered onto a pre-combusted ( $450^\circ\text{C}$  for  $> 4$  h) GF/F filter (0.7  $\mu\text{m}$  nominal pore size). Filters were folded, placed in cryovials and stored at  $-80^\circ\text{C}$  for later analysis of particulate  $^{15}\text{N}$  and DIN uptake rate calculations. Between experiments, bottles were acid washed and re-used for experiments with the same  $^{15}\text{N}$ -DIN type.

### 2.3 Chemical concentrations

160 Nitrite concentrations were measured ship-board with a spectrometer using colorimetric methods and calibrated with a standard curve bracketing the expected nitrite concentrations of samples (Strickland and Parsons, 1972). Briefly, 5 ml of sample or standard was reacted with 200  $\mu\text{l}$  each of sulfanilamide (SAN) and N-(1-Naphthyl)ethylenediamine (NED) reagents and absorbance at 543 nm was measured after 10 min of color development. The limit of detection was  $\sim 200$  nM. Ammonium concentrations were measured shipboard by fluorometry using an adapted *o*-phthalaldehyde (OPA) method (Holmes et al., 1999, as modified in Santoro  
165 201X). Standard curves were made by standard addition to a seawater matrix, with water collected from below the euphotic zone. Samples and standards were incubated using OPA reagent for  $\sim 8$  hours before measurement. The limit of detection for this method was 30 nM. Nitrate concentrations were measured against a bracketing standard curve using a WestCo SmartChem 200 Discrete Analyzer at Stanford University, with a detection limit of 85 nM and precision of 0.6  $\mu\text{M}$  (Miller and Miller, 1988; Rajaković et al., 2012).

170

### 2.4 Isotopic analyses

For estimates of ammonia oxidation, nitrite oxidation and nitrate reduction rates, the 0- and 8-h timepoints from each incubation were analyzed for  $^{15}\text{N}$  enrichment in the product pools. Product DIN was converted to nitrous oxide either by bacterial conversion  
175 using the denitrifier method (Sigman et al., 2001; McIlvin and Casciotti, 2011) or chemical conversion using the azide method (McIlvin and Altabet, 2005).

**Table 1. Tracer additions and preparation process for rate measurements**

Process	$^{15}\text{N}$ -labeled reactant	$^{15}\text{N}$ -labeled product	Prep Method
Ammonia Oxidation	$\text{NH}_4\text{Cl}$	$\text{NO}_x$	Denitrifier method
Nitrite Oxidation	$\text{NaNO}_2$	$\text{NO}_3^-$	Sulfamic treated + denitrifier method
Nitrate Reduction	$\text{KNO}_3$	$\text{NO}_2^-$	Azide method w/ carrier
Nitrite Uptake	$\text{NaNO}_2$	Particulate N	Dry and pack in tin

180 Both ammonia oxidation and nitrite oxidation measurements utilized the denitrifier method to quantify  $^{15}\text{NO}_x^-$  in the product pool. For nitrite oxidation measurements,  $\text{NO}_2^-$  in  $^{15}\text{NO}_2$ -spiked samples was removed by pre-treatment with 4% sulfamic acid solution



and 2M sodium hydroxide prior to conversion of the remaining nitrate to N<sub>2</sub>O via bacterial denitrification, resulting in analysis of nitrate-derived N<sub>2</sub>O only (Granger and Sigman, 2009). Nitrate reduction measurements utilized chemical conversion of product NO<sub>2</sub><sup>-</sup> to N<sub>2</sub>O with azide (McIlvin and Altabet, 2005). Briefly, after removal of background N<sub>2</sub>O by purging with N<sub>2</sub> gas, samples were treated with 2 M sodium azide solution in 20% acetic acid for ~30 min followed by neutralization with 6 M sodium hydroxide. The nitrite product pool in nitrate reduction samples was often highly enriched in <sup>15</sup>N due to low ambient nitrite concentrations; therefore, additional carrier NaNO<sub>2</sub> was added prior to isotopic analysis (25 μl of 200 μM NaNO<sub>2</sub> in 10 ml sample). After analysis, the isotopic composition of the carrier-diluted samples was calculated by subtracting out the known isotopic value and concentration of the added NaNO<sub>2</sub> carrier using mass balance.

Isotopic enrichment of the resulting N<sub>2</sub>O in all cases was determined using a Thermo-Finnigan Delta<sup>PLUS</sup>XP or Delta V<sup>PLUS</sup> isotope ratio mass spectrometer connected to a custom-built cryogenic purge and trap system with autosampler (PAL) (McIlvin and Casciotti, 2011). Samples were loaded into 20 ml headspace vials with volumes adjusted to achieve 20 nmoles N (for Delta V<sup>PLUS</sup>) or 40 nmoles N (Delta<sup>PLUS</sup> XP). For NO<sub>3</sub><sup>-</sup> or NO<sub>x</sub><sup>-</sup> isotope samples, δ<sup>15</sup>N and δ<sup>18</sup>O values were calibrated using nitrate isotope standards USGS32, USGS34 and USGS35 (Böhlke et al., 2003). Each run included two quality control samples (a GEOTRACES deep seawater sample and an in-house standard KNO<sub>3</sub> solution). Standards were run at 9-sample intervals, and used for correction of instrument drift. For NO<sub>2</sub><sup>-</sup> isotope samples, δ<sup>15</sup>N and δ<sup>18</sup>O values were calibrated using nitrite isotope standards RSIL-N23, N7373 and N10219 (Casciotti et al., 2007). These standards were run at ~6-sample intervals at two levels (5 and 10 nmol NO<sub>2</sub><sup>-</sup>), to correct for sample size and instrument drift. The mean analytical precision of natural abundance δ<sup>15</sup>N isotope measurements using the denitrifier method is typically less than 0.5‰, but enriched experiments often have higher standard deviations. For our tracers experiments the analytical precisions were 0.4‰, 4‰ and 0.7‰ for <sup>15</sup>NO<sub>x</sub><sup>-</sup>, <sup>15</sup>NO<sub>3</sub><sup>-</sup> and <sup>15</sup>NO<sub>2</sub><sup>-</sup> measurements, respectively.

Filters for determination of <sup>15</sup>N uptake rates were dried at 50 °C overnight and packed into tin capsules prior to shipment to the Biogeochemical Stable Isotope Facility at the University of Hawaii. Samples were analyzed on a Thermo Scientific Delta V Advantage isotope ratio mass spectrometer coupled to a Costech Instruments elemental analyzer.

## 2.5 Rate Calculations:

The rates of microbial transformations were calculated using measurements of <sup>15</sup>N enrichment in the product pool over time following Eq. (1):

$$rate_t = \frac{[^{15}N]_{p,t} - [^{15}N]_{p,t0}}{F_{r,t0} \times \Delta t}, \quad (1)$$

where <sup>15</sup>N<sub>p,t0</sub> and <sup>15</sup>N<sub>p,t</sub> are the concentrations of <sup>15</sup>N in the product at the start of the experiment (t<sub>0</sub>) and the final time point (t), respectively. The fraction of <sup>15</sup>N in the reactant N pool, F<sub>r,t0</sub> = <sup>15</sup>N/(<sup>14</sup>N+<sup>15</sup>N), includes the ambient DIN and <sup>15</sup>N tracer addition. The detection limit was calculated as the rate that can be reasonably discerned from zero. Since variation in replicate isotope measurements can be more variable at higher enrichment levels, we used the CV% for each rate process to help normalize across varied enrichment levels in our tracer experiments. The theoretical detection limits for each process were calculated from equation 1 by propagating a mean CV% increase in δ<sup>15</sup>N into the product pool. The detection limits were 0.2, 8.5 and 0.9 nM d<sup>-1</sup> for ammonia oxidation, nitrite oxidation and nitrate reduction, respectively.



220 Uptake rates were determined using particulate samples collected at the end of each experiment. Analysis of particulate samples  
by isotope ratio mass spectrometry provided particulate  $\delta^{15}\text{N}$  and the total particulate N ( $\mu\text{mol N}$ ). Uptake rates were calculated  
following a constant uptake model as discussed in Dugdale and Wilkerson (1986). The above equation (1) was slightly modified  
with the assumption that the atom fraction  $^{15}\text{N}$  of the ambient DIN reactant and initial particulate N are 0.003663, and the initial  
reactant pool was calculated from the mixture of ambient and  $^{15}\text{N}$ -labeled DIN based on mass balance.

225

Daily rates for ammonia oxidation, nitrite oxidation, nitrate reduction and nitrite uptake were calculated from hourly rates using a  
12 h:12 h dark light cycle from the dark incubation and the 8 h time point from the appropriate light level, and are reported as  $\text{nM d}^{-1}$ . Net nitrification (NetNit) rates were calculated by subtracting nitrite oxidation rate from ammonia oxidation rate. Likewise,  
for phytoplankton processes net nitrite production (NetPhy) was calculated as nitrate reduction minus nitrite uptake. Furthermore,  
230 total net nitrite production rate ( $\text{NetNO}_2^-$ ) from all four nitrite cycling processes was calculated by subtracting consumption  
processes (nitrite oxidation and nitrite uptake) from the sum of the production processes (ammonia oxidation and nitrate reduction).  
Note that the summation of rates into a net rate will be influenced by potential  $^{15}\text{N}$  enhancement occurring in each process.

## 235 2.6 Light inhibition and enhancement

235

To compare the influence of light on nitrite cycling across different source waters, a percent change in rate (R) due to light level  
was calculated for each experiment, relative to dark conditions ( $R_{\text{DK}}$ ). Percent change was calculated as a fraction relative to the  
dark incubation and multiplied by 100 ( $P_c = 100 \cdot (R - R_{\text{DK}}) / R_{\text{DK}}$ ). Calculating percent change relative to the dark rates means that  
rates from the low light treatments, which approximate the *in situ* conditions at  $\sim 1\%$  PAR, show whether the populations are  
240 inhibited or enhanced by light in their natural environment (at collection depth). Rates showing negative percent change are  
considered inhibited by light, while positive percent change values (typically phytoplankton-driven processes) were enhanced by  
increasing light level.

## 3 Results

### 3.1 Nutrients and hydrography

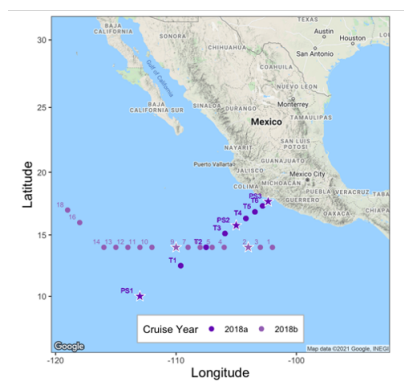
245

The coastal station (PS3) from April 2018 (SR1805) was located 12 miles from the coast with a shallow mixed layer of  $\sim 16$  m  
(Fig. 1). The depth of 1% PAR was at 31 m, and the nitracline fell within the euphotic zone. At the top of the nitracline ( $\sim 10$  m),  
light was  $\sim 13.6\%$  surface PAR. With both nitrate and light available, maximal chlorophyll concentrations reached as high as  $12.3$   
 $\text{mg m}^{-3}$  at a depth of 13 m. The PNM was at 20-30 m depth, with maximum concentrations reaching  $1.32 \mu\text{M}$ . A large secondary  
250 nitrite maximum (max  $2800 \text{ nM NO}_2^-$ ) was also detectable below  $\sim 55$  m, within the oxygen deficient zone. In contrast, the offshore  
station (PS1) had a deeper mixed layer ( $\sim 45$  m) with a nitracline beginning at 50 m. Light reached deeper into the water column,  
with 1% PAR at  $\sim 59$  m. At the offshore station, the light level at the nitracline depth was  $\sim 3.3\%$  surface PAR. Chlorophyll levels  
were lower, and reached a maximum of only  $6.4 \text{ mg m}^{-3}$  at a depth of 49 m. The PNM was at 55-60 m, with a concentration as  
high as  $1.52 \mu\text{M}$ . A secondary nitrite maximum was also detectable around 220 m at the offshore station, but a much lower nitrite  
255 accumulation was found compared to PS3 ( $< 100 \text{ nM}$ ). The central station (PS2) had a PNM nitrite concentration reaching  $620 \text{ nM}$   
situated near 65 m. The secondary nitrite maximum was large, reaching  $2200 \text{ nM}$  near 180 m. A well-defined nitracline began at  
55 m, similar to the offshore station. The PS2 chlorophyll maximum reached  $5.7 \text{ mg m}^{-3}$  at a depth of 64 m (Fig. 1, S1, Table S1).



260 During the FK180624 cruise in June 2018, Stations 2 and 9 were visited before and after a storm passed through the area, respectively. At Station 2, the primary nitrite maximum had a concentration of 766 nM at 66 m depth ( $\text{SigmaT} = 23.899 \text{ kg m}^{-3}$ ). Nitrate concentration at the depth of the nitrite maximum was  $8.4 \mu\text{M}$ . At Station 9, the primary nitrite maximum had a concentration of 390 nM at 68 m ( $\text{SigmaT}=23.13 \text{ kg m}^{-3}$ ) and the nitrate concentration at this depth was  $4.3 \mu\text{M}$  (Fig. 1, S1, Table S1).

265 **Figure 1. Map of study region showing cruise tracks from April 2018 (SR1805) and June 2018 (FK180624). Stars indicate stations where water was collected for experimental manipulations near the depth of the primary nitrite maximum.**



## 270 3.2 Experimental rate measurements

Rates for light and nitrate experiments conducted at the three processes stations (coastal PS3, central PS2, offshore PS1) during the April 2018 cruise are presented below. Experimental rates from additional stations in April 2018 and the June 2018 cruise are presented in the supplement (Fig. S2, S3, S4).

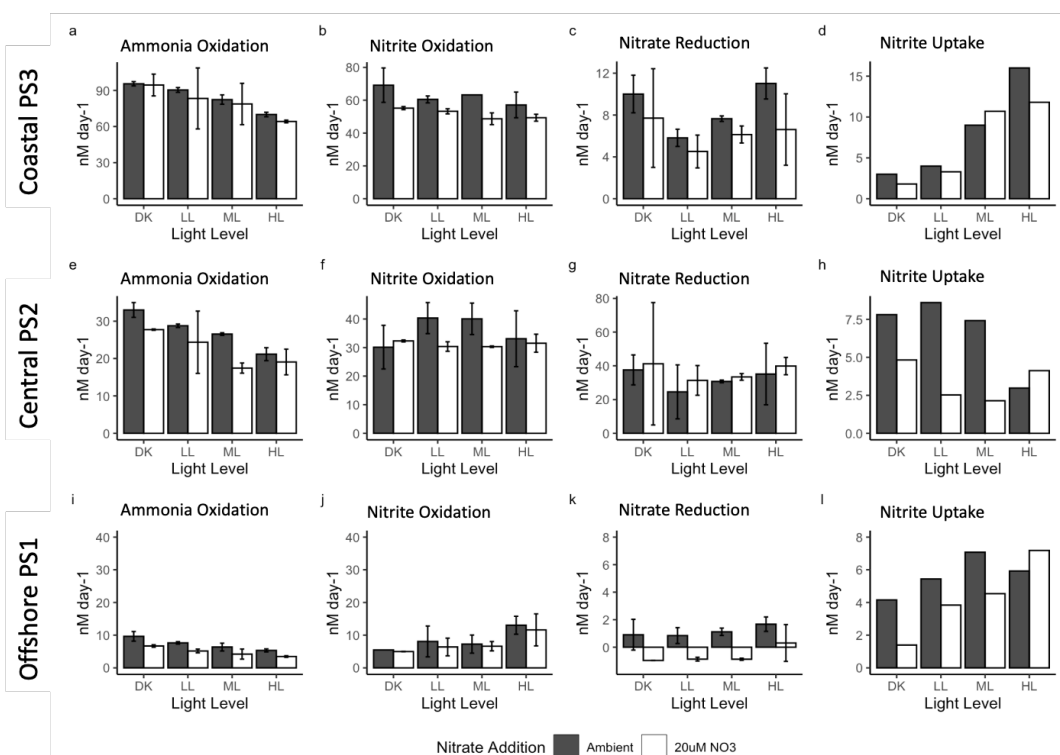
275

### 3.2.1 Coastal station (PS3)

280 At the coastal station PS3, ammonia oxidation and nitrite oxidation rates ranged from  $64 \pm 0.8$  to  $96 \pm 1.3 \text{ nM d}^{-1}$  across all experimental treatments (Fig. 2a, b). Source water for this experiment was collected at 30 m depth ( $\text{SigmaT} = 24.75 \text{ kg m}^{-3}$ ) where ambient light was  $\sim 1.4\%$  of surface irradiance (Table S2). This ambient light level corresponded to the simulated light levels in the LL deck incubators ( $\sim 1\%$  surface PAR), while ML and HL incubators were  $\sim 4\%$  surface PAR and  $\sim 20\%$  surface PAR, respectively. Addition of nitrate resulted in an increase in nitrate concentration from  $18 \mu\text{M}$  to  $37 \mu\text{M}$ .



285 **Figure 2.** Rate measurements ( $\text{nM d}^{-1}$ ) from experimental manipulation of light and nitrate using source water collected at coastal station PS3 (top row), central ODZ station PS2 (middle row) and offshore station PS1 (bottom row). Ammonia oxidation (a, e, i), nitrite oxidation (b, f, j), nitrate reduction (c, g, k) and nitrite uptake (d, h, l) are shown at each station with ambient nitrate concentration (solid bars) and  $20 \mu\text{M}$  nitrate treatment (open bars) for each light condition (dark=DK, low light=LL, medium light=ML and high light=HL). Error bars depict standard error of replicate incubations where available.



290

There were measurable rates of ammonia oxidation in all treatments, with the highest rates found in the dark ( $96 \pm 1.3 \text{ nM d}^{-1}$ ) (Fig. 2a). Rates of ammonia oxidation decreased as the light level increased from dark to the high light treatment, but even in the HL treatment, ammonia oxidation was still high ( $70 \pm 1.3 \text{ nM d}^{-1}$ ). This trend occurred in both the  $20 \mu\text{M}$   $\text{NO}_3^-$  treatment and the ambient  $\text{NO}_3^-$  treatment. In fact, duplicate experimental bottles were not statistically different between ambient and  $20 \mu\text{M}$   $\text{NO}_3^-$  treatments at PS3, except in the HL treatment (t-test p value = 0.02). Nitrite oxidation rates also declined with increasing light at PS3, but the decrease was smaller than that of ammonia oxidation. The highest nitrite oxidation rate was  $69 \pm 7.4 \text{ nM d}^{-1}$  in the DK treatment and the lowest rate was  $57 \pm 5.5 \text{ nM d}^{-1}$  in the HL treatment. Average nitrite oxidation rates in the  $20 \mu\text{M}$   $\text{NO}_3^-$  treatments were lower than the ambient treatments for each light condition, but were not statistically different in the DK and LL conditions.

295

300

Nitrate reduction rates at PS3 ranged from  $4.5 \pm 1.1$  to  $11 \pm 1 \text{ nM d}^{-1}$ , which were much lower than the nitrification rates. However, there was not a unidirectional change across light levels, as is expected for phytoplankton-driven processes. The lowest nitrate reduction rate was in the LL treatment, and rates increased in the ML and HL conditions ( $7.6 \pm 0.2 \text{ nM d}^{-1}$  and  $11 \pm 1 \text{ nM d}^{-1}$ , respectively) resulting in a positive correlation across those light levels. However, high rates were also seen in the dark incubations ( $7.7 \pm 3.3$  to  $10 \pm 1.3 \text{ nM d}^{-1}$ ), which were of similar magnitude to those in the HL condition. Trends across light levels in the  $20 \mu\text{M}$   $\text{NO}_3^-$  treatments were similar to the ambient treatment, although rates appear to be slightly lower overall. Nitrite uptake rates ranged

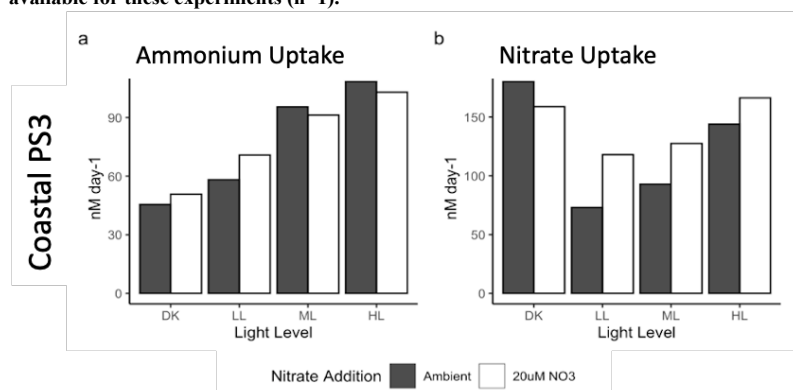
305



310

from 2 to 16  $\text{nM d}^{-1}$  and were similar in magnitude to nitrate reduction rates. The nitrite uptake rates increased steadily from the dark treatment to the highest light treatment. Typically, phytoplankton take up nitrite after, or simultaneously with, nitrate so low nitrite uptake in the presence of 18 or 37  $\mu\text{M}$  nitrate is not surprising. Further, nitrite uptake in the 20  $\mu\text{M}$   $\text{NO}_3^-$  treatments were generally lower than the ambient  $\text{NO}_3^-$ , but as there are no replicates for nitrite uptake determining statistical significance is not possible.

**Figure 3. Rates of (a) ammonium and (b) nitrate uptake from experimental manipulation of light and nitrate from source water collected at Station PS3. Ambient nitrate concentration (solid bars) and 20  $\mu\text{M}$  nitrate treatment (open bars). No replicates are available for these experiments ( $n=1$ ).**



315

At station PS3, additional measurements of DIN uptake were collected. Ammonium uptake rates were on the same order of magnitude as the ammonia oxidation rates, ranging from 45 to 108  $\text{nM d}^{-1}$  across the light conditions (Fig. 3a). However, unlike ammonia oxidation, ammonium uptake was positively correlated with light level, with the highest rates observed in the HL condition. Addition of 20  $\mu\text{M}$   $\text{NO}_3^-$  resulted in slightly higher ammonia uptake rates in the DK and LL treatments, although there were no replicates. Ambient ammonium concentrations were low, and addition of 200  $\text{nM}$   $^{15}\text{N-NH}_4^+$  tracer may have enhanced the ammonium uptake activity. Ammonium uptake rates were 6-20x higher than nitrite uptake.

320

325

Nitrate uptake rates were the highest of any measured rates, ranging from 73 to 180  $\text{nM d}^{-1}$ . The lowest rates were found in the LL treatment and increased in the ML and HL treatments (93  $\text{nM d}^{-1}$  and 144  $\text{nM d}^{-1}$ , respectively) (Fig. 3b). As observed in the nitrate reduction measurements, high nitrate uptake rates were also observed in the DK incubation and were on par with the HL treatment. In each light treatment (but not in the dark incubation), the 20  $\mu\text{M}$   $\text{NO}_3^-$  treatment led to an increase in nitrate uptake rate, although lack of replication limits determination of statistical significance.

### 3.2.2 Central station (PS2)

330

The nitrification rates at station PS2 were more moderate than at station PS3 (Fig. 2e, f). Water for these experiments was collected from 75 m depth ( $\text{SigmaT} = 25.04 \text{ kg m}^{-3}$ ), just below the nitrite maximum at PS2 where light was ~2% of surface irradiance (Table S2). Ambient nitrate concentration in the source water was 16  $\mu\text{M}$  prior to experimental nitrate addition.

335

Ammonia oxidation rates ranged from  $17 \pm 1$  to  $33 \pm 1.4 \text{ nM d}^{-1}$  across experimental treatments at station PS2 (Fig. 2e), with the highest rates in the DK incubation and the lowest rates in the HL condition. Ammonia oxidation rates appeared to be reduced in



340 the 20  $\mu\text{M}$   $\text{NO}_3^-$  treatments, especially in the ML condition, where the ambient nitrate treatment had a rate that was 1.5x higher than that with nitrate addition. Nitrite oxidation rates ranged from  $30 \pm 0.2$  to  $40 \pm 3.8$   $\text{nM d}^{-1}$  across all treatments. There was no uniform directional response of nitrite oxidation rates to increases in light level, but it is notable that the rates did not strongly decrease with increased light. The rates in ambient  $\text{NO}_3^-$  treatments were  $\sim 30$   $\text{nM d}^{-1}$  in both the DK and HL treatments, while the LL and ML treatments had ambient rates near 40  $\text{nM d}^{-1}$ . The 20  $\mu\text{M}$   $\text{NO}_3^-$  treatments all had measured nitrite oxidation rates near  $\sim 30$   $\text{nM d}^{-1}$  regardless of light level (Fig. 2f).

345 Nitrate reduction rates were  $24.6 \pm 11.3$  to  $41.2 \pm 25.7$   $\text{nM d}^{-1}$  across treatments at PS2 (Fig. 2g). Similar to station PS3, the lowest rates were in the LL treatment. The DK and HL treatments had the highest rates (near 40  $\text{nM d}^{-1}$ ), while the LL and ML treatments had lower rates. The addition of 20  $\mu\text{M}$   $\text{NO}_3^-$  did not appear to clearly change the rates of nitrate reduction at any light level. Nitrite uptake rates ranged from 2.1 to 8.6  $\text{nM d}^{-1}$  across treatments and there was no unidirectional response with increasing light level (Fig. 2h). The lowest rates were seen in the LL and ML treatments with the addition of 20  $\mu\text{M}$   $\text{NO}_3^-$ . The highest rates were also seen in the LL and ML treatments but in the ambient  $\text{NO}_3^-$  treatment. No additional nitrogen uptake rates were analyzed at station  
350 PS2.

### 3.2.3 Offshore station (PS1)

355 Rates of N transformation at station PS1 were generally lower than at PS2 and PS3 (Fig. 2i-l). Water for these experiments was collected at 60 m depth (Sigma T = 23.82  $\text{kg m}^{-3}$ ), just below the PNM feature at light levels near 0.5% of surface PAR. At 60 m depth, the ambient nitrate concentration was  $\sim 12$   $\mu\text{M}$ , so the  $\text{NO}_3^-$  addition treatment had 32  $\mu\text{M}$  (Table S2).

360 Ammonia oxidation rates ranged from  $3.5 \pm 0.2$  to  $9.7 \pm 1$   $\text{nM d}^{-1}$ , with the highest rates seen in the dark treatments. These rates followed the same light response pattern seen at the coastal station, with the highest rates in the DK, decreasing into the HL treatment. The addition of 20  $\mu\text{M}$   $\text{NO}_3^-$  to the incubations slightly decreased ammonia oxidation rates in every light treatment, although this trend was not always statistically significant. The nitrite oxidation rates at the offshore station were much lower than those measured at stations PS2 and PS3. The range in rates across treatments was  $5 \pm 0.1$  to  $13 \pm 1.9$   $\text{nM d}^{-1}$ , with the highest rates occurring in the HL condition ( $\sim 13$   $\text{nM d}^{-1}$ ). In contrast to the ammonia oxidation rates, the offshore nitrite oxidation rates increased as light increased in both the ambient and 20  $\mu\text{M}$   $\text{O}_3^-$  treatments.

365 The nitrate reduction rates at station PS1 were very low, with all rates lower than 2  $\text{nM d}^{-1}$ . The highest rate was in the HL treatment, and rates decreased to below the detection limit in many of the 20  $\mu\text{M}$   $\text{NO}_3^-$  treatments. While nitrate reduction was minimal, nitrite uptake was still active at the offshore station, with ambient rates ranging from 4.2 to 7.1  $\text{nM d}^{-1}$ . There was an increase in nitrite uptake with increasing light. Nitrate additions may have decreased nitrite uptake rates, especially in the lower light treatments. No  
370 additional nitrogen uptake rates were analyzed for station PS1.

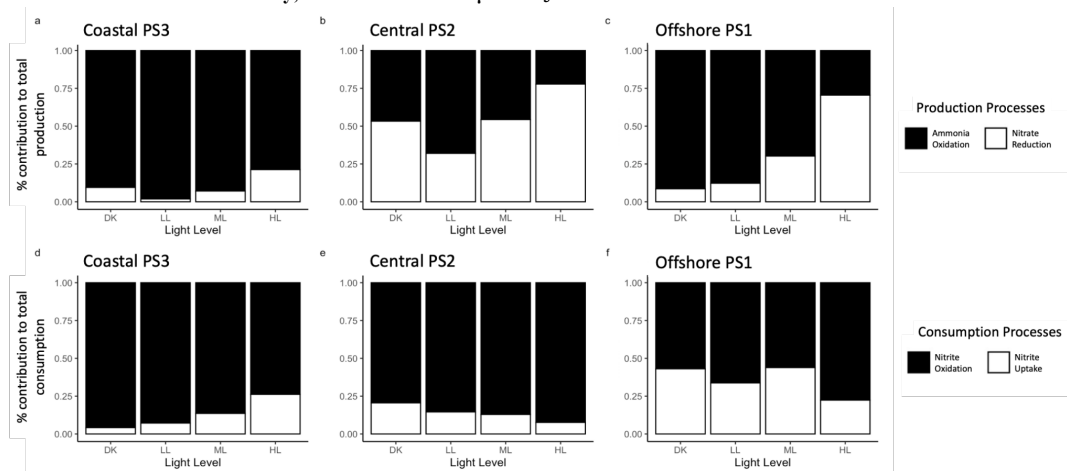
### 3.3 Light effects on the balance of nitrite production and consumption processes

375 Ammonia oxidation dominated nitrite production in the LL treatment (which is comparable to the ambient light at source water collection depth) across the three stations (Fig. 4a,b,c). At the coastal and offshore stations, ammonia oxidation comprised more than 85% of nitrite production in LL, while the percentage was smaller at the central station ( $\sim 54\%$ ). Increased light tended to



increase the relative proportion of nitrite derived from nitrate reduction. The increase in the relative contribution of nitrate reduction to nitrite production was driven by both increased nitrate reduction rates and decreased ammonia oxidation rates (Fig. 2).

380 **Figure 4. Relative contribution of production processes (top row) and consumption processes (bottom row) across light treatments at coastal PS3 (a,d), central PS2 (b,e) and offshore PS1 (c,f). Nitrification processes are black and phytoplankton processes are white. Ambient nitrate treatments only, does not include 20  $\mu\text{M}$   $\text{NO}_3^-$  treatments.**



385 Nitrite oxidation dominated nitrite consumption at all stations (Fig. 4d,e,f). In LL treatments at the coastal and central stations, nitrite oxidation was responsible for over 80% of nitrite consumption, while nitrite oxidation comprised approximately 60% of nitrite consumption at the offshore station. Increasing light did not exert a uniform directional influence: the proportion of nitrite consumed by nitrite oxidation declined at the coastal station but increased at the central and offshore stations. While nitrite oxidation comprised a larger percentage of overall consumption at the offshore station, the rates were the lowest observed (Fig.  
390 2j).

### 3.4 Percent change in rates due to light treatments

In general, ammonia oxidation rates were inhibited by increased light while phytoplankton activity was enhanced. The largest  
395 percent change ( $P_c$ ) of ammonia oxidation was seen in the HL condition at the offshore station, which reached 45% (Fig. S5i). At the coastal station, the HL condition reduced ammonia oxidation rates by 27%. Low light conditions (which correspond most closely with light level at collection depth) showed that ammonia oxidation rates within this source water microbial community are already 5-20% inhibited in the field, with the highest ambient light inhibition observed at the offshore collection depth (Fig. S5i). Nitrite oxidation rates were expected to show light inhibition as well, but only the coastal station showed clear inhibition,  
400 where  $P_c$  reached 17% in the HL treatment (Fig. S5b). At all stations, the response of nitrite oxidation to increasing light levels was not as consistent as the responses seen in ammonia oxidation rates (Fig. S5). Surprisingly, nitrite oxidation rates at the offshore station increased by >25% at all light levels relative to the dark in both ambient and 20  $\mu\text{M}$   $\text{NO}_3^-$  treatments. However, the magnitude of those rates was quite small (Fig. S5j, Fig 2j). Nitrate reduction rates were enhanced with increasing light beyond LL, but were also enhanced in the dark treatments at PS3 and PS2. Percent change in nitrite uptake was much larger than changes seen

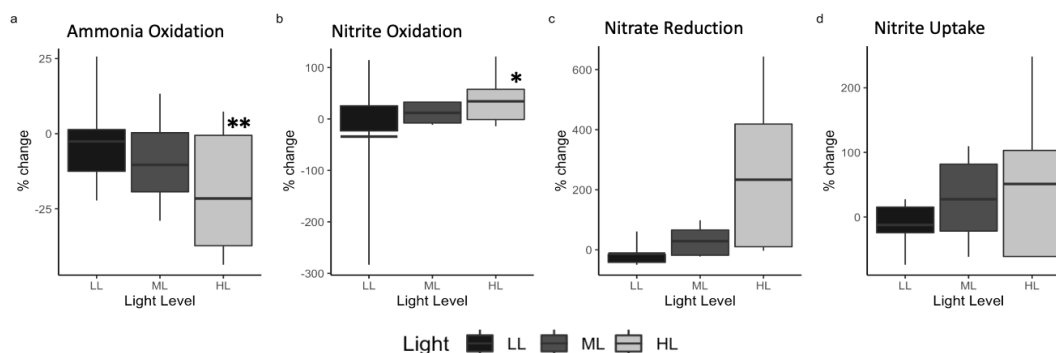


405 in nitrification rates (Fig. S5 d,h,i). The coastal station nitrite uptake rates had the largest response to increased light, with rates increasing 300-650% in the HL treatments, relative to the dark.

The  $P_c$  calculations for each station (including all cruises and  $\text{NO}_3^-$  treatments) can be summarized to look for general patterns that may hold across the region. Ammonia oxidation showed a consistent light effect across stations, where rates declined progressively  
410 in the higher light treatments. The summary plot reflects this pattern with declining percent change in rate as light level increases (Fig. 5a) with a small range in values falling within the 0.25-0.75 quantiles. The mean percent change in nitrite oxidation showed increasing rates with increasing light level across the region (Fig. 5b). However, nitrite oxidation had varying directional response to increasing light across stations (Fig. 2b,j,f, S2b, S3b, S4b,d), which contributes to the large range in  $P_c$  at LL and is obscured in the averaging of stations (Fig. S5 c,g,k).

415

**Figure 5. Summary plots of percent inhibition for each process across stations and depth by light treatment. (a) ammonia oxidation, (b) nitrite oxidation, (c) nitrate reduction, and (d) nitrite uptake at each experimental light level (LL = low light, ML = medium light, HL = high light). The horizontal bar is the mean % inhibition, the box depicts 0.25-0.75 quantiles, and lines show range to 0.95 and 0.05. Treatment different from DK with t-test, \*\*  $p < 0.01$ , \*  $p < 0.1$ .**



420

The percent change in nitrate reduction rates increased with light level, but there was high variation in the station data for this process (Fig. 5c). The range in data within the 0.25 to 0.75 quantiles is larger than for nitrification rates (~4x) especially in the HL treatments. Percent change in nitrate reduction exhibited some positive responses to decreased light (e.g., coastal station and central station) and discrepancy between the ambient and  $20 \mu\text{M NO}_3^-$  treatments (e.g., offshore and central) that contributed to the wide range of data falling within the 0.25 to 0.75 quantiles. Summarized percent change in nitrite uptake also had a wide range in the 0.25 to 0.75 quantiles, as the directional response to light was not consistent across the coastal, central, and offshore stations (nitrite uptake at the central station declined with increased light Fig. 2h). Generally, the percent change in nitrite uptake showed enhancement of rates with increased light level, and was likely driven by the strong light response seen at the coastal station (PS3; Fig. 2d). The variance in nitrate reduction and nitrite uptake rates across stations was higher than that for nitrification rates.

430

### 3.5 Net nitrite production under varying light levels

Net nitrite production from nitrification (NetNit, ammonia oxidation minus nitrite oxidation) declined with increasing light at each station (Fig. S6), consistent with field observations that NetNit generally decreases from the base of the euphotic zone towards the surface (Travis et al., 2023). The dark treatments had the largest net positive rate of nitrite production at all

435

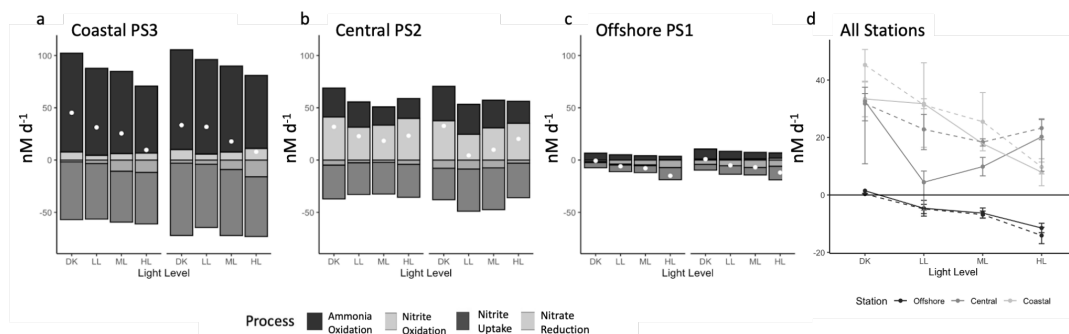


stations. Coastal station PS3, which had the largest rates of both ammonia oxidation and nitrite oxidation, also had the largest NetNit production rates with positive rates in every light treatment (Fig. S6a,d). At some stations, light level modulated NetNit enough to flip net production rates from positive to negative (Fig. S6d). Both central and offshore stations had negative NetNit values in all light treatments except DK, and had smaller contributing rate magnitudes (Fig. S6b,c). Patterns were similar in the 20  $\mu\text{M NO}_3^-$  treatment (Fig. S7)

Net nitrite production from phytoplankton (NetPhy, nitrate reduction minus nitrite uptake) declined with light at the offshore and coastal stations, and the offshore station had negative NetPhy rates at all light treatments (Fig. S8). While nitrate reduction increased with light at the coastal station, it was not large enough to offset the corresponding increase in nitrite uptake (Fig. S8a). The large positive NetPhy values at the central station were driven by very high nitrate reduction rates (Fig. S8b). These patterns held in the 20  $\mu\text{M NO}_3^-$  treatment (Fig. S9)

Overall net nitrite production rates (NetNO<sub>2</sub>) were calculated by combining all four measured nitrite cycling processes (Fig. 6). There were differences in magnitude and sign for NetNO<sub>2</sub> across the coastal, central, and offshore stations, but NetNO<sub>2</sub> generally declined with increasing light level in both the ambient and 20  $\mu\text{M NO}_3^-$  treatments. The offshore station had negative NetNO<sub>2</sub> rates at all light levels and NO<sub>3</sub><sup>-</sup> treatments except for the ambient NO<sub>3</sub><sup>-</sup> dark treatment (Fig. 6c) which had a small positive rate (<2 nM day<sup>-1</sup>). The coastal and central stations had positive NetNO<sub>2</sub> across all light and nitrate treatments (Fig. 6a,b). The 20  $\mu\text{M NO}_3^-$  treatments showed similar NetNO<sub>2</sub> patterns to the ambient treatment, except for in the LL condition.

**Figure 6. Component processes of net nitrite production (NetNO<sub>2</sub>) at each station: coastal PS3 (a) central PS2 (b) and offshore PS1 (c). Positive values represent production of nitrite and negative values represent consumption of nitrite. The net nitrite production rates at each station are presented together in panel d, and overlaid as white dots on individual station panels a,b,c. The 20  $\mu\text{M NO}_3^-$  treatments are on the left in panels a,b,c, and as dashed lines in panel d. Errors are omitted, but presented in Figure 2 for individual rates. Pooled error is calculated for NetNO<sub>2</sub> (d).**



## 4 Discussion:

### 4.1 Sensitivity of nitrification to light

Light inhibition has been used as a mechanism to help explain exclusion of ammonia-oxidizing and nitrite-oxidizing microbes from the surface ocean (Lomas and Lipschultz, 2006; Olson, 1981a). However, active nitrification has been observed in the sunlit ocean (Beman et al., 2008; Clark et al., 2008; Santoro et al., 2013; Smith et al., 2014; Francis et al., 2005; Ward, 2005) and there



is variation in apparent photosensitivity across natural communities of ammonia oxidizers (Qin et al., 2014). While decreased ambient nitrification rates have been seen above the nitrite maximum in previous work (Travis et al., 2023; Beman et al., 2012, 2013), those studies were not able to conclude that lower rates were caused by increased light level, because the microbial community and cell abundance were different at each depth measured in a vertical profile. Since the experimental design in the current study manipulated light using a single source water community, we can conclude that the declines in bulk rate measurements observed here were most likely caused directly or indirectly by changes in light intensity. Ammonia oxidation occurred in all our light treatments, including the highest level (~20% PAR), showing that light did not completely inhibit ammonia oxidation in our samples (Fig. 2).

In the field, the influence of light is overlaid on top of other factors that control the distribution of microbial populations in the natural environment, where environmental pre-conditioning and cell abundance may set the variance in the baseline rates measured in these experiments. While the magnitude of the ambient ammonia oxidation rates were indeed very different between stations (e.g., 91 and 8 nM day<sup>-1</sup> at coastal PS3 and offshore PS1, respectively), the percent light inhibition of ammonia oxidation rates when moved from ambient (~1% surface PAR) to high light treatment were similar (27-45% at all three stations).

The source water collected at each station had ambient PAR levels of 0.5~2% of surface irradiance, which were most closely approximated by the low light incubation tank (~1% PAR). Comparison of ammonia oxidation rates between the LL treatment (1% surface PAR) and the corresponding dark incubations indicates that ammonia oxidation was inhibited by 5-21% at *in situ* conditions (Fig. S5). This is consistent with prior results from the North Pacific Ocean, which showed there was 25-41% inhibition of ammonia oxidation rates at the depth of 1% surface PAR (Horak et al., 2018). This is in contrast to Smith et al. (2014) who saw little inhibition of ammonia oxidation when water from near the PNM was incubated at 50% surface PAR. Ammonia oxidation rates at the offshore station PS1 were low (8 nM d<sup>-1</sup>), already light inhibited (by 21%), and more sensitive to increased light compared to the coastal community (45 vs 26% inhibited in HL, respectively) (Fig. 2i, Fig. S5). This could result from offshore source water communities being acclimated to more stable, low light conditions compared to cells in dynamically changing light fields closer to the coast.

Nitrite oxidation rates were similar in magnitude to ammonia oxidation rates at each station, but an overarching light response for nitrite oxidation was not easy to discern. Olson et al. (1981a) showed that nitrite oxidation rates in field studies were inhibited by increases in light, possibly even more than ammonia oxidation. However, other work has suggested that nitrite oxidation may be less sensitive to increasing light intensity compared to ammonia oxidation, although recovery after photoinhibition is slower (Horak et al., 2013; Guerrero and Jones, 1996b). Oceanic profiles of nitrite oxidation activity show vertical distributions that are shaped similarly to ammonia oxidation, with maximal rates at the base of the euphotic zone and lower rates in surface waters (Travis et al., 2023; Beman et al., 2012). Overall, our data suggest that light is not the primary reason for generally low rates of nitrite oxidation in the surface ocean, but may still play a role under some conditions, in addition to substrate supply and competition for substrate within the community.

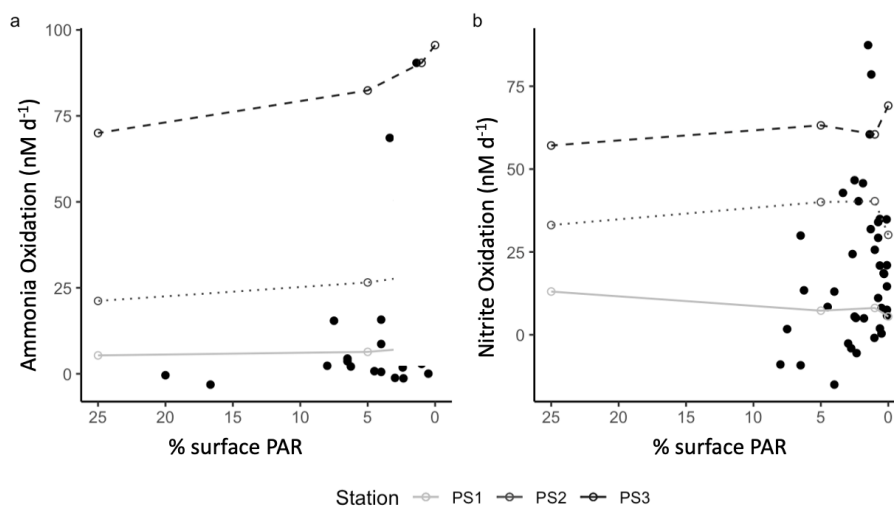
We targeted source water from PNM depths where ammonia and nitrite oxidizers are typically abundant and active (Santoro et al., 2010, 2013; Travis et al., 2023). Challenging these communities with higher light levels simulated water moving upward in the water column. In some HL treatments we measured rates of ammonia oxidation higher than those typically found in shallow, high-



light environments where ambient nitrifier abundance is low (Santoro et al., 2010; Beman et al., 2013, 2012). Figure 7 shows the measured rates from the experimental light manipulations on top of ambient measurements of ammonia oxidation and nitrite oxidation collected from a variety of depths and light conditions in the ETNP. This comparison illustrates that while nitrification rates are inhibited by light to an extent, the HL rates are much higher than ambient rates measured in communities collected from comparable light levels in the field. We argue that this is partly due to the lower abundance of nitrifying organisms in shallow waters due to chronic substrate limitation and competition. This idea is illustrated quantitatively by modeling (Zakem et al., 2018) that shows substrate concentrations (resource limitation) can control the exclusion of ammonia- and nitrite oxidizers from surface waters without invoking light inhibition.

515

**Figure 7. Experimental rates from light experiments (open circles) plotted on top of ambient measurements (closed circles) from the ETNP region. The % surface irradiance are from light levels in experimental incubations tanks, or % surface irradiance from collection depth for ambient rates. Measurements from the same source water are connected with a line across the experimental light levels tested.**



520

While it appears from our data that light inhibition alone does not exclude nitrification activity from the surface ocean, differential light responses could still help shape the balance of the two steps of nitrification vertically across the PNM feature. Decoupling of the two steps of nitrification is commonly observed in the field (Heiss and Fulweiler, 2016), whether caused by changes in mixing (Haas et al., 2021), temperature (Schaefer and Hollibaugh, 2017) or light (Olson, 1981a), and is often invoked to explain nitrite accumulation in the surface ocean. Observations of ammonia oxidation rates reaching maxima slightly shallower than nitrite oxidation maxima were initially interpreted as differential light tolerance of the two steps of nitrification in the surface ocean (Olson, 1981b). However, this vertical structure is less clear in larger datasets of paired ammonia oxidation and nitrite oxidation rates (Beman et al., 2013; Travis et al., 2023), and observational patterns cannot be causally attributed to different light tolerances.

530

Balanced nitrification may be more likely when rates of individual steps are low (e.g., PS1, Fig. 6c). In the ETNP, net nitrification (NetNit) rates have the largest imbalance around the depths of highest nitrifier activity, at the base of the euphotic zone near the PNM, but a NetNit maximum is not guaranteed at this depth (Travis et al., 2023). Moving natural microbial communities from





535 near the PNM abruptly into high light levels caused a decline in NetNit that was driven by a larger decline in ammonia oxidation  
rate compared to nitrite oxidation. For example, there was a 20 nM d<sup>-1</sup> difference in ammonia oxidation rate between LL and HL  
540 treatments at the coastal station PS3, and a corresponding decline of only 3 nM d<sup>-1</sup> in nitrite oxidation (Fig. 2). Ammonia oxidation  
appears to be more consistently inhibited in our light experiments compared to a more variable response in nitrite oxidation,  
although NetNit shows a clear decrease in rate with increasing light (Fig. 2, Fig. 6). If this pattern of net consumption of nitrite at  
higher light levels holds more generally, it could potentially help to define the upper boundary of nitrite accumulation in the PNM  
(Fig. 6d).

545 Previous work has suggested that ammonia oxidizers recover more quickly from light inhibition than nitrite oxidizers, and this  
differential recovery could also cause nitrite to accumulate at the PNM. This suggestion came from experiments done on lab  
cultures of ammonia-oxidizing bacteria, which we now know are typically less abundant than ammonia-oxidizing archaea in the  
surface ocean and contribute less to total ammonia oxidation activity (Beman et al., 2012). Additionally, *Nitrococcus maritimus*  
and *Nitrobacter sp.* were used in the light recovery experiments (Guerrero and Jones, 1996b), but we now know *Nitrospina sp.* are  
550 more abundant and active in this region. More recent work using ammonia oxidizing archaea species shows that archaea may be  
even more sensitive to light than bacterial ammonia oxidizers (Merbt et al., 2012).

550 Recovery from light inhibition can be seen in DK treatments, where ammonia oxidation rates increased when shifted from LL into  
the dark, while the directional response of nitrite oxidation rates was more variable. Moving the nitrite oxidizing community from  
low light to dark conditions only led to increased nitrite oxidation (i.e., recovery from light inhibition) at coastal station PS3, not  
at central station PS2 or offshore station PS1. Since ammonia oxidation appears to drive the patterns in NetNit from the nitrifier  
community, the focus of most studies on ammonia oxidation rate measurements may be justified. However, rates of nitrite oxidation  
555 are of similar magnitude to ammonia oxidation rates, which indicates that they are important for overall nitrite cycling in the  
surface ocean. As evidenced by the ubiquity of nitrite oxidoreductase enzyme (Nxr), more studies on the activity and environmental  
response and high variability of nitrite oxidizer communities are needed (Saito et al., 2020).

#### 560 4.2 Light sensitivity of phytoplankton nitrite release and nitrite uptake

We hypothesized that nitrate reduction would increase with increasing light, since the source water in all experiments was nitrate  
replete (>12 μM). In general, the rates of phytoplankton-driven processes were indeed enhanced by increases in light. Nitrate  
reduction rates increased slightly with light intensity across stations, but the magnitude of nitrate reduction was still much smaller  
565 than that of ammonia oxidation at the coastal and offshore stations. These incubations were done over 8 h, which is likely too short  
to capture nitrate reduction enhancement due to an increase in nitrate reductase enzymes, as the enzymes are synthesized over a  
daily cycle (Berges, 1997). The positive light response we observed likely reflects the enhanced activity of pre-existing nitrate  
reductase, and not de novo synthesis or cell growth. Therefore light response patterns in nitrate reduction will be constrained by  
the initial characteristics of the source community at each station. Nitrate reduction in this dataset was measured as an increase in  
570 nitrite released from the cell, not as assimilation into particulate matter, allowing a unique perspective on nitrite dynamics. Previous  
work has shown that nitrite release by phytoplankton is linked to nitrate uptake rates, with ~10% of nitrate uptake potentially being  
released as nitrite on average, although some estimates from N-limited or N-starved cultures had release rates upwards of 25%  
(Collos, 1998; Kiefer et al., 1976; Martinez, 1991). Enhanced nitrite release has been found in cells that were recently nitrogen



575 limited, and nitrite release appears to be a transient response to cells that are adjusting their growth rates and nitrogen assimilation enzymes to accommodate a resupply of nitrogen (Sciandra and Amara, 1994). Based on nitrate uptake measurements at the coastal station, our nitrite release rates (nitrate reduction rates) were 4-8% percent of nitrate uptake rates (Fig. S8). High rates of nitrite release >20 nM d<sup>-1</sup> (nitrate reduction measurements) were also observed at coastal stations in the ETNP in a prior study (Travis et al., 2023). For dynamic water columns, such as near coastal upwelling regions, changes in light and nitrate supply may induce more frequent episodes of nitrite release as cells frequently re-acclimate to new conditions.

580 Nitrite release from phytoplankton has been suggested as a consequence of energy balancing, where sudden increases in photon flux are dissipated by nitrate reduction while nitrite reduction is rate limiting. Diatoms may use nitrate reduction to avoid photodamage during high light events, resulting in release of nitrite or other dissolved organic nitrogen forms (Lomas et al., 1999; Lomas and Glibert, 1999). Temporary release of nitrite may occur under more moderate conditions too, when growth limitations are alleviated (light or iron), leading to a transient mismatch between energy supply and nitrogen assimilation capabilities of the  
585 phytoplankton community (Milligan and Harrison, 2000; Sciandra and Amara, 1994).

Interestingly, increased rates of nitrate reduction were also seen in the dark incubations (coastal station PS3 and central station PS2) where we would not expect phytoplankton to require photoprotective mechanisms or have excess energy supply. The elevated nitrate reduction rates seen in both the DK and HL conditions (compared to LL) may reflect the activity of two separate  
590 physiological mechanisms controlling nitrite release. While nitrate and nitrite reduction are both typically light dependent processes, depending on the enzymatic catalysis of N substrate with 2 or 6 electrons respectively, many algae are capable of nitrate uptake and assimilation in the dark without active photosynthesis. Diatoms are known to continue high rates of nitrate assimilation in the dark after daytime access to high light conditions (Clark et al., 2002).

595 Nitrate reduction is often the rate limiting step in nitrate assimilation, as evidenced by the accumulation of nitrate within phytoplankton cells compared to nitrite rarely accumulating (Dortch et al., 1984) and that nitrite reductase enzyme (NiR) activity is typically higher than nitrate reductase enzyme (NR) in nutrient replete cells (Milligan and Harrison, 2000). Milligan and Harrison (2000) witnessed a decline in NiR enzyme activity and an increase in nitrite efflux from diatoms during conditions when photosynthetically produced reductant was low, suggesting that nitrite reduction can become the rate limiting step under reduced  
600 reductant availability. This situation could occur chronically during low light or in the dark. Nitrite release due to incomplete nitrate assimilation during periods of light-limitation has also been observed in diatoms by Vacarro and Ryther (1960). Further investigation into the mechanisms and transient conditions for nitrite release in the dark are needed.

Nitrite uptake was also observed to be light-dependent, with nitrite uptake rates generally increasing with light (Fig. 2). Ambient  
605 nitrite uptake rates were similar in magnitude between coastal and offshore stations, but the HL treatment appeared to enhance nitrite uptake more at the coastal station (3-fold vs 2-fold). This change in bulk rate may be partially explained by higher chlorophyll concentrations in the coastal station source water. At the coastal station, nitrite uptake in the dark treatment did not increase alongside the increased nitrate reduction, suggesting that nitrite uptake is regulated separately from nitrate uptake/reduction and does not simply “ride-along” with nitrate uptake.

610



Phytoplankton cannot be generalized as simply net consumers or net producers of nitrite across stations and light levels, as NetPhy (nitrate reduction minus nitrite uptake) varied from positive (net producing) to negative (net consuming) between stations and between light treatments at a single station (Fig. S8, S9). When NetPhy declined clearly with increasing light, it was driven by the strong increase in nitrite uptake rates (Fig. S8a). Interestingly, nitrate reduction rates (nitrite release) were much higher at station PS2 than the other two stations, resulting in positive NetPhy across all light treatments (Fig. S8b, S9b). However, chlorophyll was not significantly more abundant at PS2; in fact, PS3 had the largest chlorophyll maximum. It is possible, instead, that the phytoplankton community at PS2 had a different species composition than the other stations causing larger nitrite release rates. The lack of stability in the water column chlorophyll profiles collected over the repeated casts from station PS2 is also suggestive of fluctuating conditions at this station that could cause physiological responses that stimulate nitrite release (Fig S1).

615  
620

#### 4.3 Net community nitrite production in response to light

At all stations there is a general unidirectional light response, where community NetNO<sub>2</sub> declines with increasing light (Fig. 6d). This correlates spatially with the upper slope of the PNM, where nitrite concentrations in the ETNP decline precipitously moving upward toward the surface. The coastal station samples consistently showed net positive NetNO<sub>2</sub> across the light treatments and the offshore station showed mostly net consumption of nitrite; however, we observed higher nitrite accumulation at the offshore station (800 nM vs 470 nM) (Fig. 8 and Table S2). This discrepancy may be due to temporal mismatch between an instantaneous rate measurement from a single day and the time-integrated accumulation of nitrite observed at the PNM.

625  
630  
635  
640

In a prior study, production of nitrite was dominated by ammonia oxidation below the PNM and shifted to a higher contribution from phytoplankton above the PNM (Travis et al., 2023). The light experiments show how an increase in light can cause a relative shift in the balance between ammonia oxidation and nitrate reduction, with phytoplankton contributing a larger percentage under higher light (Fig. 4). However, there is variation between stations in whether nitrate reduction becomes the dominant production process, which likely depends on the microbial population. Consumption of nitrite around the PNM is driven by nitrite oxidation in the ETNP (Travis et al., 2023). Here, nitrite oxidation remained the dominant nitrite consumption process across all stations and light levels, even when nitrite uptake has an increasing response to increasing light (Fig. 4). Sato et al. (2022) incubated PNM water in low light and high light conditions, and concluded from decreases in nitrite concentration that nitrite was not released by phytoplankton in the eastern Indian Ocean. However, we see that the response of individual nitrite cycling processes (such as increases in nitrate reduction/nitrite release) can be obscured when summed into a net nitrite production rate.

645

Source water was collected at the same relative PNM depth at both the coastal and offshore stations to allow comparison of response dynamics. However, attributes of the source water and community such as cell abundance, nitrogen and light acclimation history and substrate availability are not exactly the same at each station. Responses in our light experiments are thus overlain on variations in source water characteristics. Chlorophyll concentrations were higher at the coastal station PS3 compared to offshore station PS1 (~3.5 vs. 0.4 mg m<sup>-3</sup>) (Table S1). Slightly higher rates of bulk nitrate reduction and nitrite uptake at the coast may be explainable by higher chlorophyll concentration, but significantly higher ammonia oxidation rates at the coastal station cannot be explained by higher ammonia oxidizer abundance (*amoA* gene abundance shown in Table S2, Frey et al., 2023). The coastal station PS3 source water was collected from a depth with ambient light level of 1.4% surface irradiance, while the offshore source community was collected from a depth with 0.5% surface irradiance. The slightly higher light acclimation level of coastal ammonia oxidizers may



650 explain why light inhibition was lower at the coast compared to offshore (Fig. S5). Additionally, the coastal station PS3 source  
water had slightly higher nitrate and ammonium concentrations compared to offshore. Work by Xu et al. (2019) showed that light  
inhibition of ammonia oxidation occurred irrespective of substrate limitation or saturation, so variation in source water ammonium  
or enhancement due to ammonium tracer addition should not have interfered with the observed light response.

#### 655 4.4 Role of nitrate in stimulating or suppressing nitrite accumulation

The accumulation of nitrite at the base of the euphotic zone has been spatially correlated with the nitracline, suggesting a  
relationship between nitrate and nitrite cycling (Herbland and Voituriez, 1979; Travis et al., 2023). Of the microbial processes that  
mediate nitrite accumulation in the PNM, only nitrate reduction by phytoplankton is directly dependent on nitrate as a substrate.  
660 Nitrate is a key nitrogen source for phytoplankton growth, and its presence has been shown to influence the nitrogen physiology  
and regulation of cells (Berges, 1997; Fernández et al., 2009). Nitrite release by phytoplankton has been connected to nitrate  
availability and uptake, where nitrite release rates can be anywhere from 5-30% of nitrate uptake depending on light levels (Olson  
et al., 1980; Collos, 1998). Wada and Hattori (1971) showed that nitrite production increases as nitrate concentration increases.  
Our experimental addition of 20  $\mu\text{M NO}_3^-$  did not clearly enhance nitrate reduction as might be expected from these earlier studies  
665 (Fig. 2, Olson et al., 1980; Collos, 1998), and nitrate reduction at PS3 and PS1 actually declined with nitrate addition. This lack of  
rate enhancement may be explained by the *in situ* nutrient status of source phytoplankton across experiments, as source water was  
collected on the underslope of the PNM, solidly in the nitracline, and initial nitrate concentrations for these experiments ranged  
between 7.5-19.6  $\mu\text{M}$  (Table S2). Sciandra and Amara (1994) suggested that nitrite release is a transient response that occurs when  
nitrate uptake suddenly increases, either by increase in N-substrate availability or light. The nitrate-replete condition of microbes  
670 collected from these depths may have prevented a large response to additional 20  $\mu\text{M NO}_3^-$ , as nitrate was likely not limiting for  
growth or activity. Nitrite uptake might also be expected to increase with the addition of nitrate, as nitrate uptake into many  
phytoplankton cells is mediated by NRT2 transporters that can take up both  $\text{NO}_3^-$  and  $\text{NO}_2^-$  (Sanz-Luque et al., 2015). However,  
even though nitrate uptake increased with nitrate addition (at PS3, Fig 3b), nitrite uptake was lower in most of the  $\text{NO}_3^-$  addition  
treatments (Fig. 2).

675 An indirect influence of nitrate on nitrification has been suggested, whereby nitrate-based phytoplankton growth eventually  
supplies ammonium substrate via grazing and regeneration (Mackey et al., 2011), or by mediating ammonium availability through  
reduced competition for DIN resources (Smith et al., 2014; Wan et al., 2018; Xu et al., 2019). However, in our 20  $\mu\text{M NO}_3^-$  addition  
experiments, we did not observe an increase in ammonia oxidation rates at any of the SR1805 stations (Fig. 2, S4). In fact, many  
680 ammonia oxidation rates declined slightly with nitrate addition. While nitrate uptake rates at the coastal station PS3 did increase  
slightly with nitrate addition (Fig. 3b), the corresponding ammonium uptake rates declined only at higher light levels (Fig. 3a), and  
no corresponding increase in ammonia oxidation was observed. It is possible that an 8 h incubation is not long enough to reflect  
the cascade of adjustments required to result in increased ammonia oxidation rates.

685 Oligotrophic phytoplankton communities have adapted to low DIN conditions, and typically maintain low  $K_s$  values and high  $V_{\text{max}}$   
values for ammonium uptake (MacIsaac and Dugdale, 1969, 1972). Xu et al. (2019) compared substrate kinetics of ammonia  
oxidation and ammonium uptake, and confirmed that phytoplankton are more competitive for ammonium substrates at low DIN  
and higher light intensities. Perhaps further work on the enzymatic responses of nitrate reductase, nitrite reductase, glutamine



690 synthetase and ammonia monooxygenase during nitrate intrusion would clarify the interaction between microbial nitrogen  
physiologies near the PNM. Overall, nitrate additions did not appear to significantly alter NetNO<sub>2</sub> across stations.

#### 4.5 Insights into the formation and maintenance of a PNM

695 Increased light intensity modulated individual microbial processes to different extents and led to changes in net nitrite production  
as well as changes in relative contributions to nitrite production and consumption. Generally, we found that increased light levels  
cause declines in rates of ammonia oxidation and increases in phytoplankton activity. The experimental design used in this study,  
with discrete changes in light condition, most closely mimics dynamic conditions in coastal waters or dramatic mixing events such  
as storms. Net nitrite production at the offshore station is unlikely to be controlled by dramatic changes in light field, as the  
community is acclimated to more stable conditions, and is less likely to experience disturbances. We saw the strongest pre-existing  
700 light inhibition of nitrification rates from this offshore community, as well as the strongest response to increases in light (Fig. S5).  
While ammonia oxidation rates were also inhibited by high light at the coastal station, the ambient rates were large enough that a  
50% decline in rates still allowed ~60 nM d<sup>-1</sup> of ammonia oxidation even when light was increased to 20% surface PAR. The 30  
nM d<sup>-1</sup> difference between DK and HL ammonia oxidation rates at the coastal station was measured over an 8 h incubation,  
suggesting that the microbial response to light perturbations can be quite fast and large enough to switch NetNO<sub>2</sub> from positive to  
705 negative (Fig. 6). However, the observed response to changing light is dependent on the starting community.

Short term light inhibition does not entirely exclude nitrification from the surface ocean. Horak et al. (2018) also tested ammonia  
oxidation rates of PNM communities under increased light conditions and determined that light was a critical control of ammonia  
oxidation in the surface ocean, sometimes eliminating ammonia oxidation completely at high light levels. However, the ammonia  
710 oxidation rates measured in the central north Pacific Ocean (<4 nM d<sup>-1</sup>) were lower than the ambient rates in our ETNP light  
experiments (8-90 nM d<sup>-1</sup>), supporting the idea that initial community is an important determinant of how strongly a light  
perturbation will affect rates. Our lowest ambient rates were at offshore station PS1 and showed the highest percentage of light  
inhibition compared to the other stations with higher ammonia oxidation rates (Fig 2i, S5). While high light does partially inhibit  
rates, ultimately ammonia oxidizers may be excluded from surface oceans due to lack of substrate, low growth rates and/or  
715 sustained light inhibition that occurs over time scales longer than our 8 h incubations.

Changes in phytoplankton activity at the coastal and central stations showed that nitrite release via nitrate reduction has a  
complicated response to light. We observed increased nitrite release when cells were exposed to both increased light as well as  
removal of light. Interestingly, release of nitrite by phytoplankton under both low light and high light conditions has been  
720 documented in the literature. Our dataset suggests that both mechanisms may be simultaneously relevant to PNM formation in the  
ETNP, although ammonia oxidation still dominates nitrite production in the PNM. The increased responsiveness of coastal  
phytoplankton activity to changes in light confirm that dynamic coastal waters provide opportunity for larger phytoplankton  
contributions to nitrite cycling. However, the highest rates of nitrate reduction were observed at station PS2, showing that highest  
nitrite release rates are not always linked to stations with the highest chlorophyll concentration, but rather species composition or  
725 environmental conditions and disturbance history.



## 5 Conclusions

Our experimental data clearly show the influence of light level on both the individual nitrite cycling processes around the PNM feature as well as on net nitrite production rates. Each step of nitrification was independently sensitive to light, with ammonia oxidation having the clearest declining trend with increased light level and nitrite oxidation rate sometimes showing an increase with light level. Nitrification imbalance (NetNit) also declined with light, reflecting the differential responses to light intensity of the two steps of nitrification, with the highest potential for net nitrite production at the lowest light levels. Additionally, based on the difference in rates between dark incubation and low light treatments, nitrification rates near the depth of the PNM are already inhibited by light. Net phytoplankton production of nitrite (NetPhy) was variable across stations and light treatments, showing that phytoplankton can be both net producers and consumers of nitrite under different conditions. In combination, the net response of the whole microbial community varied from net nitrite producing to net nitrite consuming across stations and light levels, but NetNO<sub>2</sub> showed a clear declining trend with increases in light for each microbial community tested (Fig. S6d). Ammonia oxidation was a critical nitrite production mechanism at all stations, but we saw evidence of significant contributions from nitrate reduction at central station PS2. While abrupt perturbations in light can influence net nitrite cycling rates, the starting community influences baseline rates and limits response potential. Substrate availability and average light conditions that control microbial abundance and physiology may have more influence on the variance of nitrite concentrations near the PNM, and studies investigating nitrite cycling on longer timescales closer to the nitrite residence time may provide more insight. With the potential for warming and increased stratification of the oceans resulting from climate change, increased stability of the light environment may control the balance of nitrite cycling processes in the primary nitrite maximum.

745



## References

- Beman, J. M., Popp, B. N., and Francis, C. A.: Molecular and biogeochemical evidence for ammonia oxidation by marine Crenarchaeota in the Gulf of California, *The ISME journal*, 2, 429–441, <https://doi.org/10.1038/ismej.2007.118>, 2008.
- 750 Beman, J. M., Popp, B. N., and Alford, S. E.: Quantification of ammonia oxidation rates and ammonia-oxidizing archaea and bacteria at high resolution in the Gulf of California and eastern tropical North Pacific Ocean, *Limnol. Oceanogr.*, 57, 711–726, <https://doi.org/10.4319/lo.2012.57.3.0711>, 2012.
- Beman, J. M., Shih, J. L., and Popp, B. N.: Nitrite oxidation in the upper water column and oxygen minimum zone of the eastern tropical North Pacific Ocean, *The ISME journal*, 7, 2192–2205, <https://doi.org/10.1038/ismej.2013.96>, 2013.
- 755 Berges, J.: Miniview: algal nitrate reductases, *Eur. Jour. Phyc.*, 32, 3–8, <https://doi.org/10.1080/09541449710001719315>, 1997.
- Berges, J. A. and Harrison, P.: Nitrate reductase activity quantitatively predicts the rate of nitrate incorporation under steady state light limitation: a revised assay and characterization of the enzyme in three species of marine phytoplankton, *Limnol. Oceanogr.*, 40, 82–93, <https://doi.org/10.4319/lo.1995.40.1.0082>, 1995.
- 760 Berges, J. A., Cochlan, W. P., and Harrison, P. J.: Laboratory and field responses of algal nitrate reductase to diel periodicity in irradiance, nitrate exhaustion, and the presence of ammonium, *Mar. Ecol. Prog. Ser.*, 259–269, <https://doi.org/10.3354/meps124259>, 1995.
- Böhlke, J. K., Mroczkowski, S. J., and Coplen, T. B.: Oxygen isotopes in nitrate: new reference materials for  $^{18}\text{O}$ :  $^{17}\text{O}$ :  $^{16}\text{O}$  measurements and observations on nitrate-water equilibration: Reference materials for O-isotopes in nitrate, *Rapid Commun. Mass Spectrom.*, 17, 1835–1846, <https://doi.org/10.1002/rcm.1123>, 2003.
- 765 Brandhorst, W.: Nitrite Accumulation in the North-East Tropical Pacific, *Nature*, 182, 679–679, <https://doi.org/10.1038/182679a0>, 1958.
- Carlucci, A. F., Hartwig, E. O., and Bowes, P. M.: Biological production of nitrite in seawater, *Mar. Biol.*, 7, 161–166, <https://doi.org/10.1007/BF00354921>, 1970.
- 770 Casciotti, K. L., Böhlke, J. K., McIlvin, M. R., Mroczkowski, S. J., and Hannon, J. E.: Oxygen isotopes in nitrite: analysis, calibration, and equilibration, *Anal. Chem.*, 79, 2427–2436, <https://doi.org/10.1021/ac061598h>, 2007.
- Clark, D. R., Flynn, K. J., and Owens, N. J.: The large capacity for dark nitrate-assimilation in diatoms may overcome nitrate limitation of growth, *New Phytologist*, 155, 101–108, 2002.
- Clark, D. R., Rees, A. P., and Joint, I.: Ammonium regeneration and nitrification rates in the oligotrophic Atlantic Ocean: Implications for new production estimates, *Limnology and Oceanography*, 53, 52–62, 2008.
- 775 Collos, Y.: Nitrate uptake, nitrite release and uptake, and new production estimates, *Mar. Eco. Progress*, 171, 293–301, <https://doi.org/10.3354/meps171293>, 1998.
- Collos, Y. and Berges, J.: Nitrogen metabolism in phytoplankton, Oxford, UK: Eolss Publishers, 2003.
- Dortch, Q., Clayton, J., Thoresen, S., and Ahmed, S.: Species differences in accumulation of nitrogen pools in phytoplankton, *Marine Biology*, 81, 237–250, 1984.
- 780 Fernández, E., Llamas, Á., and Galván, A.: Chapter 3 - Nitrogen Assimilation and its Regulation, in: *The Chlamydomonas Sourcebook (Second Edition)*, edited by: Harris, E. H., Stern, D. B., and Witman, G. B., Academic Press, London, 69–113, <https://doi.org/10.1016/B978-0-12-370873-1.00011-3>, 2009.
- 785 Francis, C. A., Roberts, K. J., Beman, J. M., Santoro, A. E., and Oakley, B. B.: Ubiquity and diversity of ammonia-oxidizing archaea in water columns and sediments of the ocean, *Proceedings of the National Academy of Sciences of the United States of America*, 102, 14683–14688, <https://doi.org/10.1073/pnas.0506625102>, 2005.



- Frey, C., Sun, X., Szemlerski, L., Casciotti, K. L., Garcia-Robledo, E., Jayakumar, A., Kelly, C. L., Lehmann, M. F., and Ward, B. B.: Kinetics of nitrous oxide production from ammonia oxidation in the Eastern Tropical North Pacific, *Limnology & Oceanography*, 68, 424–438, <https://doi.org/10.1002/lno.12283>, 2023.
- 790 Granger, J. and Sigman, D. M.: Removal of nitrite with sulfamic acid for nitrate N and O isotope analysis with the denitrifier method, *Rapid Communications in Mass Spectrometry*, 23, 3753–3762, <https://doi.org/10.1002/rcm.4307>, 2009.
- Guerrero, M. A. and Jones, R. D.: Photoinhibition of marine nitrifying bacteria. I. Wavelength-dependent response, *Marine Ecology Progress Series*, 141, 183–192, <https://doi.org/10.3354/meps141183>, 1996a.
- Guerrero, M. A. and Jones, R. D.: Photoinhibition of marine nitrifying bacteria. II. Dark recovery after monochromatic or polychromatic irradiation, *Marine Ecology Progress Series*, 141, 193–198, <https://doi.org/10.3354/meps141193>, 1996b.
- 795 Haas, S., Robicheau, B. M., Rakshit, S., Tolman, J., Algar, C. K., LaRoche, J., and Wallace, D. W. R.: Physical mixing in coastal waters controls and decouples nitrification via biomass dilution, *Proc Natl Acad Sci USA*, 118, e2004877118, <https://doi.org/10.1073/pnas.2004877118>, 2021.
- Hattori, A. and Wada, E.: Nitrite distribution and its regulating processes in the equatorial Pacific Ocean, *Deep Sea Res.*, 18, 557–568, [https://doi.org/10.1016/0011-7471\(71\)90122-7](https://doi.org/10.1016/0011-7471(71)90122-7), 1971.
- 800 Heiss, E. M. and Fulweiler, R. W.: Coastal water column ammonium and nitrite oxidation are decoupled in summer, *Estuarine, Coastal and Shelf Science*, 178, 110–119, <https://doi.org/10.1016/j.ecss.2016.06.002>, 2016.
- Herbland, A. and Voituriez, B.: Hydrological structure analysis for estimating the primary production in the tropical Atlantic Ocean, *Journal of Marine Research*, 37, 87–101, 1979.
- 805 Holmes, R. M., Aminot, A., K erouel, R., Hooker, B. A., and Peterson, B. J.: A simple and precise method for measuring ammonium in marine and freshwater ecosystems, *Canadian Journal of Fisheries and Aquatic Sciences*, 56, 1801–1808, <https://doi.org/10.1139/f99-128>, 1999.
- Hooper, A. B. and Terry, K. R.: Photoinactivation of ammonia oxidation in *Nitrosomonas*, *Journal of Bacteriology*, 119, 899–906, 1974.
- 810 Horak, R. E. A., Qin, W., Schauer, A. J., Armbrust, E. V., Ingalls, A. E., Moffett, J. W., Stahl, D. A., and Devol, A. H.: Ammonia oxidation kinetics and temperature sensitivity of a natural marine community dominated by Archaea, *ISME J*, 7, 2023–2033, 2013.
- Horak, R. E. A., Qin, W., Bertagnolli, A. D., Nelson, A., Heal, K. R., Han, H., Heller, M., Schauer, A. J., Jeffrey, W. H., Armbrust, E. V., Moffett, J. W., Ingalls, A. E., Stahl, D. A., and Devol, A. H.: Relative impacts of light, temperature, and reactive oxygen on thaumarchaeal ammonia oxidation in the North Pacific Ocean, *Limnology and Oceanography*, 63, 741–757, <https://doi.org/10.1002/lno.10665>, 2018.
- 815 Horrigan, S. and Springer, A.: Oceanic and estuarine ammonium oxidation: effects of light, *Limnology and Oceanography*, 35, 479–482, 1990.
- Kelly, C. L., Travis, N. M., Baya, P. A., and Casciotti, K. L.: Quantifying Nitrous Oxide Cycling Regimes in the Eastern Tropical North Pacific Ocean With Isotopomer Analysis, *Global Biogeochem Cycles*, 35, <https://doi.org/10.1029/2020GB006637>, 2021.
- 820 Kiefer, D., Olson, R., and Holm-Hansen, O.: Another look at the nitrite and chlorophyll maxima in the central North Pacific, in: *Deep Sea Research and Oceanographic Abstracts*, 1199–1208, [https://doi.org/10.1016/0011-7471\(76\)90895-0](https://doi.org/10.1016/0011-7471(76)90895-0), 1976.
- Lomas, M., Rumpley, C., and Gilbert, P.: Photoregulated NO<sub>3</sub><sup>-</sup> reduction: contrasting patterns of NO<sub>2</sub><sup>-</sup> and NH<sub>4</sub><sup>+</sup> release by diatoms and dinoflagellates following a shift to high light, in: *American Society of limnology and oceanography, Spring Meeting*, Santa Fe, New M xico, USA, 1999.
- 825





- Lomas, M. W. and Glibert, P. M.: Temperature regulation of nitrate uptake: A novel hypothesis about nitrate uptake and reduction in cool-water diatoms, *Limnol. Oceanogr.*, 44, 556–572, <https://doi.org/10.4319/lo.1999.44.3.0556>, 1999.
- Lomas, M. W. and Glibert, P. M.: Comparisons of nitrate uptake, storage, and reduction in marine diatoms and flagellates, *Journal of Phycology*, 36, 903–913, <https://doi.org/10.1046/j.1529-8817.2000.99029.x>, 2000.
- 830 Lomas, M. W. and Lipschultz, F.: Forming the primary nitrite maximum: Nitrifiers or phytoplankton?, *Limnology and Oceanography*, 51, 2453–2467, <https://doi.org/10.4319/lo.2006.51.5.2453>, 2006.
- MacIsaac, J. J. and Dugdale, R. C.: The kinetics of nitrate and ammonia uptake by natural populations of marine phytoplankton, *Deep Sea Research and Oceanographic Abstracts*, 16, 45–57, [https://doi.org/10.1016/0011-7471\(69\)90049-7](https://doi.org/10.1016/0011-7471(69)90049-7), 1969.
- 835 MacIsaac, J. J. and Dugdale, R. C.: Interactions of light and inorganic nitrogen in controlling nitrogen uptake in the sea, in: *Deep Sea Research and Oceanographic Abstracts*, 209–232, 1972.
- Mackey, K. R., Bristow, L., Parks, D. R., Altabet, M. A., Post, A. F., and Paytan, A.: The influence of light on nitrogen cycling and the primary nitrite maximum in a seasonally stratified sea, *Prog. Ocean.*, 91, 545–560, <https://doi.org/10.1016/j.pocean.2011.09.001>, 2011.
- 840 Martinez, R.: Transient nitrate uptake and assimilation in *Skeletonema costatum* cultures subject to nitrate starvation under low irradiance, *Journal of plankton research*, 13, 499–512, 1991.
- McIlvin, M. R. and Altabet, M. A.: Chemical conversion of nitrate and nitrite to nitrous oxide for nitrogen and oxygen isotopic analysis in freshwater and seawater, *Analytical Chemistry*, 77, 5589–5595, <https://doi.org/10.1021/ac050528s>, 2005.
- McIlvin, M. R. and Casciotti, K. L.: Technical updates to the bacterial method for nitrate isotopic analyses, *Analytical chemistry*, 83, 1850–1856, <https://doi.org/10.1021/ac1028984>, 2011.
- 845 Meeder, E., Mackey, K. R., Paytan, A., Shaked, Y., Iluz, D., Stambler, N., Rivlin, T., Post, A. F., and Lazar, B.: Nitrite dynamics in the open ocean—clues from seasonal and diurnal variations, *Marine Ecology Progress Series*, 453, <https://doi.org/10.3354/meps09525>, 2012.
- 850 Merbt, S. N., Stahl, D. A., Casamayor, E. O., Martí, E., Nicol, G. W., and Prosser, J. I.: Differential photoinhibition of bacterial and archaeal ammonia oxidation, *FEMS microbiology letters*, 327, 41–46, <https://doi.org/10.1111/j.1574-6968.2011.02457.x>, 2012.
- Miller, J. and Miller, J.: *Statistics for Analytical Chemistry*, 2nd, Ed., John Wiley & Sons, NY, 1988.
- Milligan, A. J. and Harrison, P. J.: Effects of non-steady-state iron limitation on nitrogen assimilatory enzymes in the marine diatom *thalassiosira weissflogii* (BACILLARIOPHYCEAE), *Journal of Phycology*, 36, 78–86, 2000.
- 855 Olson, R. J.: Differential photoinhibition of marine nitrifying bacteria: a possible mechanism for the formation of the primary nitrite maximum, *J. mar. Res.*, 39, 227–238, 1981a.
- Olson, R. J.: N-15 tracer studies of the primary nitrite maximum, *Journal of Marine Research*, 39, 203–226, 1981b.
- Olson, R. J., Soohoo, J. B., and Kiefer, D. A.: Steady-state Growth of the Marine Diatom *Thalassiosira pseudonana* uncoupled kinetics of nitrate uptake and nitrite production, *Plant physiology*, 66, 383–389, 1980.
- 860 Qin, W., Amin, S. A., Martens-Habben, W., Walker, C. B., Urakawa, H., Devol, A. H., Ingalls, A. E., Moffett, J. W., Armbrust, E. V., and Stahl, D. A.: Marine ammonia-oxidizing archaeal isolates display obligate mixotrophy and wide ecotypic variation, *Proc. Natl. Acad. Sci. U.S.A.*, 111, 12504–12509, <https://doi.org/10.1073/pnas.1324115111>, 2014.
- Rajaković, L. V., Marković, D. D., Rajaković-Ognjanović, V. N., and Antanasijević, D. Z.: The approaches for estimation of limit of detection for ICP-MS trace analysis of arsenic, *Talanta*, 102, 79–87, 2012.



- 865 Saito, M. A., McIlvin, M. R., Moran, D. M., Santoro, A. E., Dupont, C. L., Rafter, P. A., Saunders, J. K., Kaul, D., Lamborg, C. H., Westley, M., Valois, F., and Waterbury, J. B.: Abundant nitrite-oxidizing metalloenzymes in the mesopelagic zone of the tropical Pacific Ocean, *Nat. Geosci.*, 13, 355–362, <https://doi.org/10.1038/s41561-020-0565-6>, 2020.
- Santoro, A., Sakamoto, C., Smith, J., Plant, J., Gehman, A., Worden, A., Johnson, K., Francis, C., and Casciotti, K.: Measurements of nitrite production in and around the primary nitrite maximum in the central California Current, *Biogeosciences*, 10, 7395–7410, 2013.
- 870 Santoro, A. E., Casciotti, K. L., and Francis, C. A.: Activity, abundance and diversity of nitrifying archaea and bacteria in the central California Current, *Environmental Microbiology*, 12, 1989–2006, 2010.
- Sanz-Luque, E., Chamizo-Ampudia, A., Llamas, A., Galvan, A., and Fernandez, E.: Understanding nitrate assimilation and its regulation in microalgae, *Frontiers in Plant Science*, 6, <https://doi.org/10.3389/fpls.2015.00899>, 2015.
- 875 Sato, M., Hirata, K., Shiozaki, T., and Takeda, S.: Effects of iron and light on microbial nitrogen cycles in the primary nitrite maxima of the eastern Indian Ocean, *Deep Sea Research Part I: Oceanographic Research Papers*, 185, 103808, <https://doi.org/10.1016/j.dsr.2022.103808>, 2022.
- Schaefer, S. C. and Hollibaugh, J. T.: Temperature Decouples Ammonium and Nitrite Oxidation in Coastal Waters, *Environmental Science & Technology*, 51, 3157–3164, <https://doi.org/10.1021/acs.est.6b03483>, 2017.
- 880 Sciandra, A. and Amara, R.: Effects of nitrogen limitation on growth and nitrite excretion rates of the dinoflagellate *Prorocentrum minimum*, *Mar. Ecol. Prog. Ser.*, 105, 301–309, <https://doi.org/MEPS.105:301-309>, 1994.
- Smith, J. M., Chavez, F. P., and Francis, C. A.: Ammonium uptake by phytoplankton regulates nitrification in the sunlit ocean, *PloS one*, 9, e108173, <https://doi.org/10.1371/journal.pone.0108173>, 2014.
- Strickland, J. D. and Parsons, T. R.: A practical handbook of seawater analysis, 2nd ed., Fisheries Research Board of Canada, Ottawa, Canada, 310 pp., 1972.
- 885 Sun, X., Frey, C., Garcia-Robledo, E., Jayakumar, A., and Ward, B. B.: Microbial niche differentiation explains nitrite oxidation in marine oxygen minimum zones, *ISME J*, 15, 1317–1329, <https://doi.org/10.1038/s41396-020-00852-3>, 2021.
- Travis, N. M., Kelly, C. L., Mulholland, M. R., and Casciotti, K. L.: Nitrite cycling in the primary nitrite maxima of the eastern tropical North Pacific, *Biogeosciences*, 20, 325–347, <https://doi.org/10.5194/bg-20-325-2023>, 2023.
- 890 Vaccaro, R. F. and Ryther, J. H.: Marine Phytoplankton and the Distribution of Nitrite in the Sea\*, *ICES Journal of Marine Science*, 25, 260–271, <https://doi.org/10.1093/icesjms/25.3.260>, 1960.
- Wada, E. and Hattori, A.: Nitrite metabolism in the euphotic layer of the central North Pacific Ocean, *Limnol. Oceanogr.*, 16, 766–772, <https://doi.org/10.4319/lo.1971.16.5.0766>, 1971.
- 895 Wan, X. S., Sheng, H.-X., Dai, M., Zhang, Y., Shi, D., Trull, T. W., Zhu, Y., Lomas, M. W., and Kao, S.-J.: Ambient nitrate switches the ammonium consumption pathway in the euphotic ocean, *Nat Commun*, 9, 915, <https://doi.org/10.1038/s41467-018-03363-0>, 2018.
- Wan, X. S., Sheng, H., Dai, M., Church, M. J., Zou, W., Li, X., Hutchins, D. A., Ward, B. B., and Kao, S.: Phytoplankton-nitrifier interactions control the geographic distribution of nitrite in the upper ocean, *Global Biogeochem Cycles*, <https://doi.org/10.1029/2021GB007072>, 2021.
- 900 Ward, B. B.: Light and substrate concentration relationships with marine ammonium assimilation and oxidation rates, *Marine Chem*, 16, 301–316, [https://doi.org/10.1016/0304-4203\(85\)90052-0](https://doi.org/10.1016/0304-4203(85)90052-0), 1985.
- Ward, B. B.: Temporal variability in nitrification rates and related biogeochemical factors in Monterey Bay, California, USA, *Mar Ecol Prog Ser*, 292, 97–109, <https://doi.org/10.3354/meps292097>, 2005.



905 Xu, M. N., Li, X., Shi, D., Zhang, Y., Dai, M., Huang, T., Glibert, P. M., and Kao, S.: Coupled effect of substrate and light on assimilation and oxidation of regenerated nitrogen in the euphotic ocean, *Limnol Oceanogr*, 64, 1270–1283, <https://doi.org/10.1002/lno.11114>, 2019.

Zakem, E. J., Al-Haj, A., Church, M. J., van Dijken, G. L., Dutkiewicz, S., Foster, S. Q., Fulweiler, R. W., Mills, M. M., and Follows, M. J.: Ecological control of nitrite in the upper ocean, *Nature Communications*, 9, <https://doi.org/10.1038/s41467-018-03553-w>, 2018.

910 **Author contributions:**

Experimental design, and major data collection efforts, data processing/analysis and writing were conducted by NMT. Significant support during data collection was provided by CLK, with additional contributions during data analyses and manuscript editing. KLC was involved in initial project design, laboratory analysis, data investigations and manuscript writing.

**Acknowledgements:**

915 Thank you to the Captains and crew of the R/V Sally Ride and the R/V Falkor for assistance and support at sea. Thank you to Chief Scientists Bess Ward (SR1805) and Andrew Babbin (FK180624) for their efforts in support of this work. Thanks also to Anabelle Baya for mass spectrometer assistance during isotope analyses. This work is supported by NSF awards OCE 1657868 and OCE 1736756 to KLC. N. Travis was partly supported by the Stanford Department of Earth System Science. C. Kelly was partly supported by an NSF Graduate Research Fellowship.

920 **Data availability:**

Cruise data can be accessed on BCO-DMO for SR1805 (<https://www.bco-dmo.org/dataset/854091>, last access: 1 January 2022, Ward and Casciotti, 2021) and for FK180624 (<https://www.bco-dmo.org/dataset/832389>, last access: 1 January 2022, Babbin et al., 2021). Corresponding rate measurements can be accessed on the Stanford Digital Repository (<https://purl.stanford.edu/ds821fj1220>, Travis et al., 2023).

925

**Competing interests:**

The contact author has declared that none of the authors has any competing interests.